4

LA 20 P
30792

INTENSIFICATION OF RESEARCH IN PRIORITY AREAS (IRPA) GRANT (PROJET NO. 03-02-05-2129 EA005)

COMPREHENSIVE REPORT

Project title: **Design of natural fiber-reinforced composite pallets**

Project leader: Dr. Mani Maran a/l Ratnam
School of Mechanical Engineering
Universiti Sains Malaysia,
Engineering Campus,
14300 Nibong Tebal,
Penang.

Co-researchers: Assoc. Prof. Dr. Abdul Khalil Shawkataly
School of Industrial Technology,
Universiti Sains Malaysia,
11800 Penang.

Assoc. Prof. Dr. Ishak Abd. Azid
School of Mechanical Engineering
Universiti Sains Malaysia,
Engineering Campus,
14300 Nibong Tebal,
Penang.

Duration of project: 1 September 2002 – 31 August 2005

Contents:

1. Introduction

1.1 Project Description

The objective of this project is to design and develop pallets made from natural fiber-reinforced composite materials. Pallets are use widely in the materials handling industry for transporting goods. Most pallets are made from wood that have various drawbacks, such as deterioration when used in extreme whether conditions, fungal attack, boards that break easily and low reusability. Extensive use of wood in pallet manufacture leads to high timber consumption, thus leading to other environmental problems.

Various designs and types of pallet are fabricated to meet different load bearing requirements, such as stringer-class pallets, block-class pallets, panel deck pallets, grocery industry four-way pallets etc (Figure 1). The pallets are designed so that products/goods can be easily retrieved and delivered using lift truck such as forklift or pallet jack. Most of the pallets are made of wood and nearly 400 million wood pallets are produced annually, accounting for 86 percent of all pallets sold.

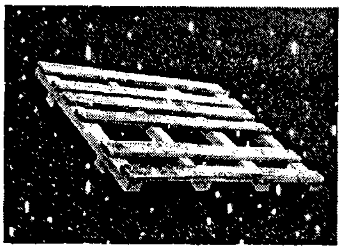

Single face, flush stringer, 4-way entry

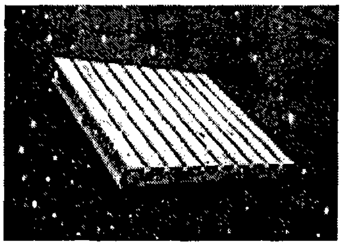

Double face, reversible, stringer-class wood pallet

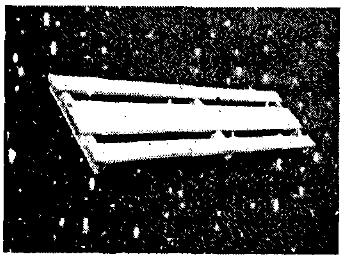

Single face, flush stringer, 2-way entry wood pallet

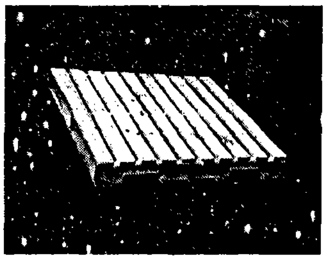

Double face, non-reversible, 4-way notched wood pallet

Figure 1. Various types of wood pallets.

Although they are cheap, wood pallets have some inherent disadvantages compared to non-wood pallets such as plastic or metal pallets. Wood can undergo degradation due to environment factors such as heat, moisture and fungal attack especially when used under extreme whether conditions. The method of fastening various members of a wood pallet, usually by nailing or screwing, does not guarantee a reliable performance of the pallet over a period of time. Also excessive use of wood in pallet production requires many trees to be cut down, causing forest depletion and thus leading to other environment problems.

In view of the disadvantages of wood pallets, pallet manufacturers worldwide use metals, such as steel or aluminum and plastics in place of wood. Plastic pallets that are of lightweight, high strength and durability are increasingly used instead of conventional wood pallets. However, plastic pallets are more expensive than the wood pallets by three to five times, although this cost can be offset by the number of trips and shipments that can be achieved with plastic pallets compared to wood pallets. One main disadvantage of using plastic pallets is that non-biodegradable plastic is hazardous to human and environment when disposed by burning.

The interest in using natural fibers, such as sisal, oil-palm empty fruit bunch fibers, coconut husk fibers, jute fibers and wood fiber as reinforcement in plastics has increased dramatically for the past few years. Compared to man-made fibers such as glass and carbon fibers, natural fibers have several advantages. For instance, natural fibers are easily available, have low density, and are biodegradable. They are renewable raw materials and have relatively high strength-to-weight ratio. Although pallets made from natural fiber-reinforced composite pallets could undergo degradation due to attack by microorganisms, the resistance to microbiological degradation can be improved by means of chemical modification.

With the current emphasis on recycling and environmentally friendly approaches to manufacturing, composite pallets made from waste fibers and recycled plastic (polypropylene) have significant potential for use as raw material in the fabrication of pallets for the material handling industry. This research was proposed to develop such materials and use them in the design and fabrication of the pallets.

1.2 Project Activities

The activities carried out in this project can be summarized as follows:

Stage 1: Preparation of composite material and mechanical property testing

Wood sawdust fibers were process into fillers of various sizes and used to prepare the composite material. Recycled plastic, namely polypropylene was used as the matrix. Various tests were carried out to characterize the material in terms of mechanical and physical properties.

Stage 2: Design of pallet using computer modeling

Several designs of the pallet were generated using computer modeling software. Particular attention was given to the method of fastening the various members of the structure.

Stage 3: Finite element analysis

The model was imported into a finite element software package for automeshing, constraint and load assignment and complete analysis of strain and deformation. Static concentrated and distributed loads were used in the analysis. The model was optimized to reduce the quantity of material used in the model.

Stage 4: Fabrication of pallet

Several one-fifth scale models and a prototype of the pallet were fabricated using the composite material based on established standard design specifications as used in the modeling. An optimum design determined from the modeling and finite element analysis was used for the fabrication.

Stage 5: Fastener study

The objective of this part of the research is to find a suitable fastening method, mechanical fastener types and sizes for used in assembly of the stringer-class natural filler composite pallet.

Stage 6: Experimental and loading rig development

This stage of the work involves the design of the experimental setup, image acquisition and loading rig to apply the shadow moiré method to measure the pallet deformation. The loading rig comprises fixtures to support the structure and load the pallet with point and distributed loads.

Stage 7: Moiré fringe analysis

Suitable image processing and analysis operations were performed to extract displacement information from the moiré fringes. The analysis was carried out on a plate to verify the measurement and later applied to the pallet model under static load. The measurement results were presented in three-dimensional graphical form for comparison with the finite element predictions.

Stage 8: Comparison between measurement and FEA results

The displacement data from experiments was compared with those from FEA. Discrepancies between the two results were studied to determine the issues involved in the computer modeling and analysis of the composite pallet.

The various stages of the work are reported in the papers published and the theses produced from this research. Detailed reports on these are available in the Appendix.

1.3 Project Benefits

Through this research, composite materials made from waste wood sawdust filler and recycled plastic have been developed and their various mechanical and physical properties have been characterized. Based on this material, one-fifth scale models and full-size pallets have been developed. Computer modeling was used to determine the load capacities of these pallets.

The output of this research has significant application in the materials handling industry to replace plastic and wood pallets. The pallets developed in this research have high load capacity, durability and lower cost compared to plastic pallets.

1.4 Project Duration

This project started in September 2002 and was completed in August 2005, that is, for duration of three years. An additional six months was required to carry out the study to determine suitable fastener types for use in the assembly of the composite pallet.

1.5 Approved Grant Amount

The total amount approved under the IRPA grant for this project is RM 170,200.00

1.6 Project Cost

The total amount spent for this project was RM 163,276.18. Out of this, RM 35,982.00 was used to purchase the equipment approved in the application.

2. Project Contribution/Achievement

2.1 Theses and publications

The contribution of this research in terms of theses and publications are as follows:

MSc thesis:

1) MSc thesis titled: An experimental and finite element analysis of the static deformation of natural fiber-composite pallet – Khoo Teng Seng (February 2006).

2) MSc thesis titled: Recycled polypropylene filled wood saw dust composites – Sharifah Shahnaz Syed Bakar (August 2005).

Journal papers:

1) M.M.Ratnam, J.H.Lim, H.P.S. Abdul Khalil, 'Study of 3-D deformation of a pallet using phase-shift shadow moiré and FEA', *Experimental Mechanics*, Vol. 45, No. 1, p9-17 (2005).

2) Abdul Khalil H.P.S., S. Shahanaz, M. M. Ratnam, "Recycle Polypropylene (RPP) - Wood Saw Dust (WSD) Composites-Part 1: The Effect of Different Filler Size and Filler Loading on Mechanical and Water Absorption Properties", *Journal of Reinforced Plastics and Composites* (in press – 2006).

3) Abdul Khalil H.P.S., S. Shahanaz, M. M. Ratnam, A..M. Issam, F. Ahmad, N.A.N. Fuaad, 'Recycled Polypropylene (PP) – wood saw dust (WSD) composites: The effect of acetylation on mechanical and water absorption properties', Wood Korea (in press – 2006).

Conference papers:

1) S.B. Shahnaz, H.P.S. Abdul Khalil, R. Mani Maran, 'Recycle polypropylene (PP) – wood saw dust composites: The effect of acetylation on mechanical and water absorption properties', *Advanced Technology Congress*, May 20-21, 2003, Putrajaya, Selangor.

2) Sharifah Shahnaz, H.P.S. Abdul Khalil, Mani Maran Ratnam, 'The Effect Of Anhydride Modifications On Mechanical Properties And Water Absorption Of Recycled Polypropylene-Wood Saw Dust Composites', *The 17th Symposium of Malaysian Chemical Engineers 2003* (SOMChE 2003) 29-30th December 2003, Penang.

3) Teng Seng Khoo, Mani Maran Ratnam, H.P.S. Abdul Khalil, 'Comparison of the mechanical properties of various wood filler based polypropylene composites and study of load ratings of composite pallets using FEA', *2nd Colloquium on Postgraduate Research: National Postgraduate Colloquium on Materials, Minerals and Polymers* (MAMIP 2004), 7-8 October 2004, Penang.

4) S.B.Shahnaz, H.P.S.Abdul Khalil, R. Mani Maran, Khoo Teng Seng, 'Recycled polypropylene (PP) – wood saw dust composites: Mechanical and water

absorption properties', 2^{nd} *Colloquium on Postgraduate Research: National Postgraduate Colloquium on Materials, Minerals and Polymers* (MAMIP 2004), 7-8 October 2004, Penang.

5) Noriman N.Z, Abdul Khalil H.P.S., Ahmad M.N., Bustaman M.R, Ratnam M.M., 'Mechanical and physical properties of carbon black and activated carbon composites', *ATCi 2005, Conference on Bio-Engineering*, Dec 6-8. 2005, Putrajaya, Malaysia

6) Sharifah Shahnaz S.A.B. Abdul Khalil H.P.S, Ratnam M.M., Faiz Ahmad, Nik Fuaad N.A., 'Recycle polypropylene (rpp) – wood saw dust (wsd) composites - Part 1: The effect of different filler size and filler loading on mechanical and water absorption properties', *ATCi 2005. Conference on Bio-Engineering*, Dec 6-8, 2005, Putrajaya, Malaysia

Copies of the full papers are available in the Appendix attached to this report.

2.2 Award

A bronze medal was won for the product titled 'Pallets from recycled plastic and waste natural fibers' in ITEX2003 held from 16-18 May 2003 in Kuala Lumpur. (Copy of certificate included in the Appendix)

2.3 Pallets from recycled plastic and wood saw dust

The pallets made using the composite material developed in this research are shown in Figure 2. Detailed description of the design, modeling and load capacities are given in the reports attached in the Appendix.

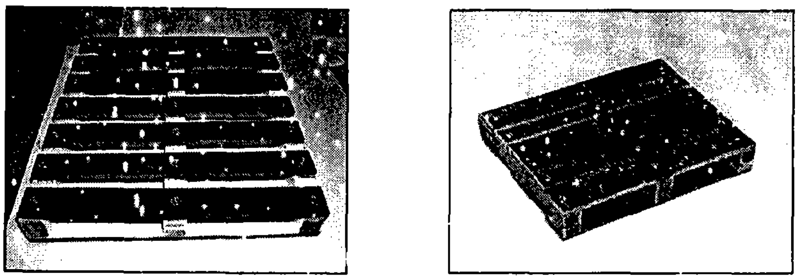

Figure 2. Pallets developed in this researach.

3. Conclusion

In this project, composite materials made from recycled plastic and wood saw dust have been successfully developed. The mechanical and physical properties of this material were characterized and documented in thesis, journal and conference papers. The material was used in the fabrication of one-fifth scale and full-size pallets. The pallets were designed and analyzed using solid modeling and finite element software.

The output of this research is expected to have significant commercial potential. The basic technologies relating to material formulation and manufacture, pallet design and optimization are available. However, to realize the commercialization aspect, additional funding is required to fabricate several full-size pallets and to design and develop a pallet testing rig.

4. Acknowledgement

We would like to convey our sincere thanks to the Ministry of Science, Technology and Innovation for the offer of the IRPA grant that has enabled this research to be carried out and completed successfully.

Report prepared by:

....
Dr. Mani Maran a/l Ratnam (Project leader)
Associate Professor,
School of Mechanical Engineering,
Engineering Campus,
Universiti Sains Malaysia,
14300 Nibong Tebal,
Penang.

Recycle Polypropylene (RPP) – Wood Saw Dust (WSD) Composites – Part 1: The Effect of Different Filler Size and Filler Loading on Mechanical and Water Absorption Properties

H. P. S. ABDUL KHALIL* AND S. A. B. SHARIFAH SHAHNAZ
School of Industrial Technology, Universiti Sains Malaysia
11800 Penang, Malaysia

M. M. RATNAM
School of Mechanical Engineering, Engineering Campus
Universiti Sains Malaysia, 14300 Nibong Tebal, Penang, Malaysia

FAIZ AHMAD
Mechanical Engineering Department, Universiti Teknologi PETRONAS
31750 Tronoh, Perak, Malaysia

N. A. NIK FUAAD
School of Housing, Building and Planning, Universiti Sains Malaysia
11800 Penang, Malaysia

ABSTRACT: The compounding of recycled polypropylene (RPP) and wood saw dust (WSD) are done by five different filler loading (0, 10, 20, 30, 40, and 50%) with three WSD filler size (100, 212, and 300 μm). The composites are mixed and extruded using Haake Rheodrive 500 twin screw extruder. The mechanical and water absorption properties of composites are characterized accordingly. Results shows that composites with smaller particle size (100 μm) have remarkably higher properties compared to others (212 and 300 μm). Composites filled up to 30% WSD exhibits improved mechanical properties but the value dramatically decreased above 30% filler loading. The evidence of fiber–matrix interphase is analyzed using scanning electron microscope (SEM).

KEY WORDS: recycled polypropylene (RPP), wood saw dust (WSD), mechanical properties, water absorption properties, thermoplastic composites.

*Author to whom correspondence should be addressed. E-mail: akhalil@usm.my

0731-6844/0?/00 0001–13 $10.00/0 DOI: 10.1177/073168440?062060

[Ver: A3B2 8.07r/W] [8.12.2005–3:33pm] [1–1?] [Page No. 1] FIRST PROOFS {Sage}Jrp/JRP-62060.3d (JRP) Paper: JRP-62060 Keyword

INTRODUCTION

A SIGNIFICANT AMOUNT of research has recently focused on wood-based polymer (either thermoset, thermoplastic or elastomers) composites [1–4]. The review of various articles on the utilization of lignocellulosic fibers as filler in thermoplastic composites has shown the possible application of these material groups. Promising technology is merging for using recycled plastic with low-grade filler, such as wood saw dust (WSD) to produce high performance composites product [1]. The burgeoning of interests in the development of products having unique properties and cost benefits from the combination of wood and other raw materials, such as plastics, or concrete as a matrix evolved in the 1990s [4].

Malaysia is one of the developing countries which are abundantly endowed with agricultural resources like vegetable oils, lignocellulosic fibers, and scraps from the wood-based industry. There are vast quantities of lignocellulosic fibers available as a waste in Malaysia. Natural fiber has very high potential as composites filler as they have properties that are comparable to synthetic filler. Kenaf, wood fiber, empty fruit bunches (EFB), and coir has shown good performance as composites filler [5]. Moreover, they seem to be economically attractive, particularly light weight, have low densities, easily processed, non-hazardous, has high durability, renewable, and their availability is more or less unlimited [6–9]. Wood saw dust is a high quality wood waste and is a side product of the wood processing industry. It has high potential as composites filler in polymer thermoplastic and has been used to replace synthetic fibers [1,4], which are difficult to recycle. Wood saw dust has fibrous structures, which function as a reinforcement in plastic. In addition to being biodegradable and recyclable, lignocellulosic material also provide good insulating and mechanical properties when used as reinforcement filler. However, lignocellulosic fibers have very low resistance on environmental influences. The hydrophilic nature of lignocellulosic fibers which limits the compatibility between filler and matrix, also causes dimensional instability when exposed to moisture. They are also susceptible to decomposition by fungi, bacteria, and insects, have high inflammability and have degradable surface when exposed to light (photo-sensitiveness) [10].

However, these disadvantages have been overcome as lignocellulosics were used as a filler in thermoplastic composites [2,4]. The properties of composites come directly from their structure, there is a through mixture of the filler and plastic. The matrix effectively coats the particle as a thin layer, as shown in Figure 1.

The combination of plastic and lignocellulosic filler has caused the escalating cost of raw material and energy, light weight high performance materials product. In this study, recycled polypropylene (RPP) was used as it can accept various types of fillers and

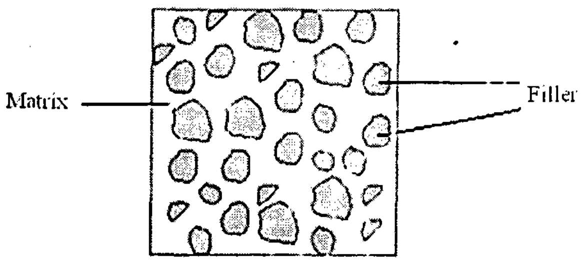

Figure 1. The fillers are completely coated with plastic.

reinforcements, such as glass fibers, glass sphere, talc, asbestos, mica, wallastonite, calcium carbonate, and silica [11]. Polypropylene (PP) belongs to polyolefin family, has a linear structure that can be melted and remolded a few times. The PP is also available abundantly as a waste material, causing environmental problems [12]. In order to reduce this problem, PP can be recycled at their end life phase, producing new value added product with lower production costs. Recycling has been continually improved and new technology have been developed which enables wastes to be reused [12,13]. The PP has high softening point and its mechanical properties are constant at ambient temperature, has dimensional consistency, impact resistance, and high strength-to-weight ratios [14]. The objective of this study is to determine the effect of different filler loading (0, 10, 20, 30, 40, and 50%) and filler size (100, 212, and 300 μm) on the mechanical and water absorption properties of the composites.

MATERIALS AND METHODS

Materials Preparation

Wood saw dust was obtained from a Chuah Joo sawmill. The WSD was sieved and segregated accordingly to 3 sizes (100, 212, and 300 μm) using Restch Test Sieve. Each meshed WSD was dried in an oven to remove the moisture prior to Soxhlet extraction in the next process. The drying phase was necessary to protect wood from excessive drying stresses that cause defects and degradation. Soxhlet apparatus was prepared using 4 : 1 : 1 mixture of toluene, ethanol, and acetone for 3 h. The extracted WSD was then dried in oven at 105°C overnight before being cooled in dessicator over silica gel. The RPP used was supplied by local plastic manufacturer. The RPP was crushed using crusher model S4301 into smaller particle size for processing.

Mixing Process

The composites were prepared using 5 different filler loading (0, 10, 20, 30, 40, and 50% w/w) for each filler size (100, 212, and 300 μm). The mixture of WSD and RPP was compounded using twin screw extruder model Haake Rheodrive 500. The extruder was pre-heated to 180°C. The composite mixture was added gradually into the hopper and observed to ensure that the WSD blended well with RPP and averted clogging of the mixture in the extruder. The extrusion strands were cooled before being palletized using.

Compression Molding

Palletized composites were weighed according to the volume of the mold. Pallets were spread in the mold that has been covered with a transparency to prevent the melting pallet from sticking to the mold. The mold was then pressed for 20 min at 190°C at 8 tonnes using Carver Laboratory Press model 'M'.

Testing

Three types of mechanical testing were conducted in this study, as followed from the previous study [5]. Tensile and flexural tests of the composites specimens were carried out according to ASTM D3139 and ASTM D 790 standards respectively, using an

Instron Universal Testing Machine Model 1114. The Charpy impact tests were carried out on un-notched samples according to ASTM D256 Standard, using an Impact Pendulum Tester (Zwick) Model 5101. A minimum of 20 samples were tested in each case. Water absorption property of the composites was determined according to ASTM D570. The samples were weighed and immersed in water up to 100 days. Then they were removed, blotted with tissue paper to remove the excess water on surface, and the weight was recorded. The water absorption was calculated according to the Equation 1 [15].

$$\text{Water absorption, WA}(\%) = \frac{M_2 - M_1}{M_1} \times 100 \qquad (1)$$

where: M_2 is the mass of the sample after immersion (g); M_1 is the mass of the same sample before immersion (g).

RESULTS AND DISCUSSION

Figures 2–6 show the tensile properties of WSD–RPP composites. Figure 2 shows that tensile strength decreases as filler loading increased, except at 20% WSD loading where the value dropped slightly. The reduction is possibly due to overheating during compression molding, which effected the burning of WSD and weaken the strength of the composite. Higher filler loading did not improved the strength of the composites, in contrast reduced the properties. The phenomenon occurred because of poor matrix–filler bonding as WSD loading increased. Similar trends also showed with the increment of filler size. Smaller particle (100 μm) size showed better reinforcing properties compared to the bigger filler size (212 and 300 μm). Smaller WSD size tends to blend well with RPP matrix as they have bigger surface area, which enables RPP matrix to bind entirely with WSD particle. The higher tensile strength of 15.54 MPa was gained by composites with 10% filler loading

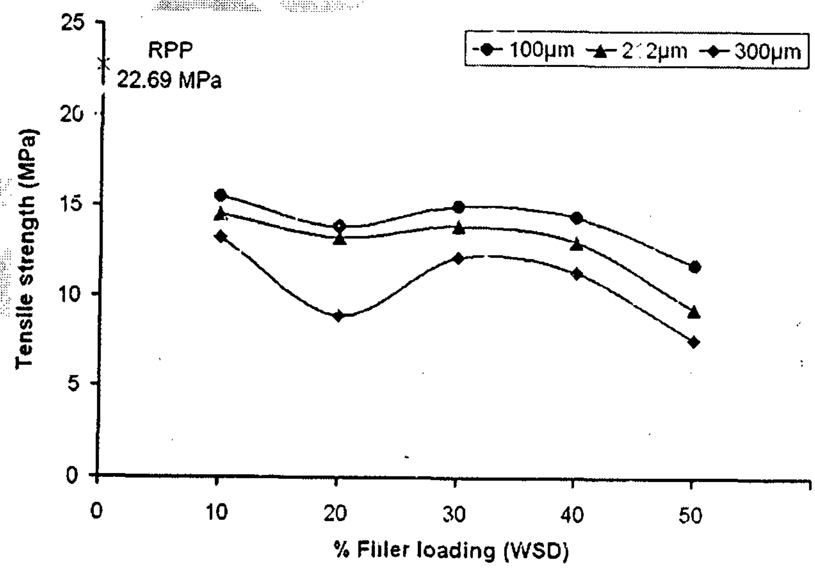

Figure 2. Effect of filler size and filler loading on tensile strength of WSD–RPP composites.

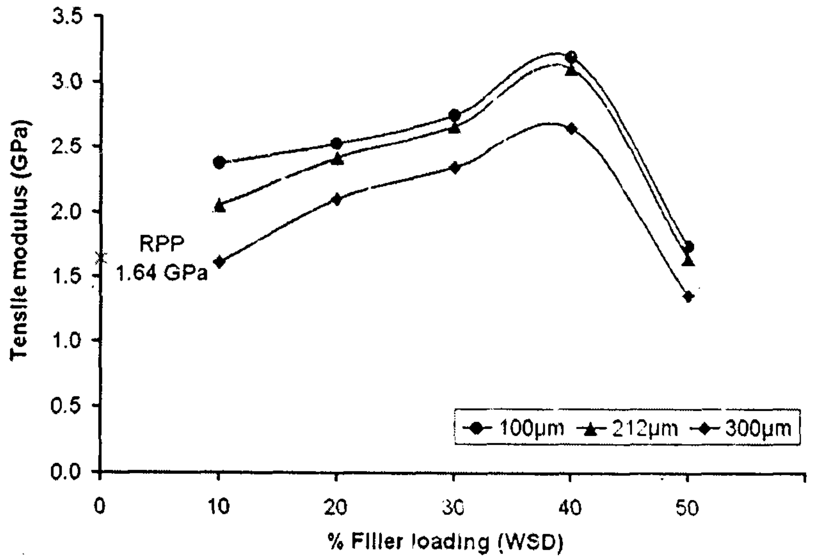

Figure 3. Effect of filler size and filler loading on tensile modulus of WSD-RPP composites.

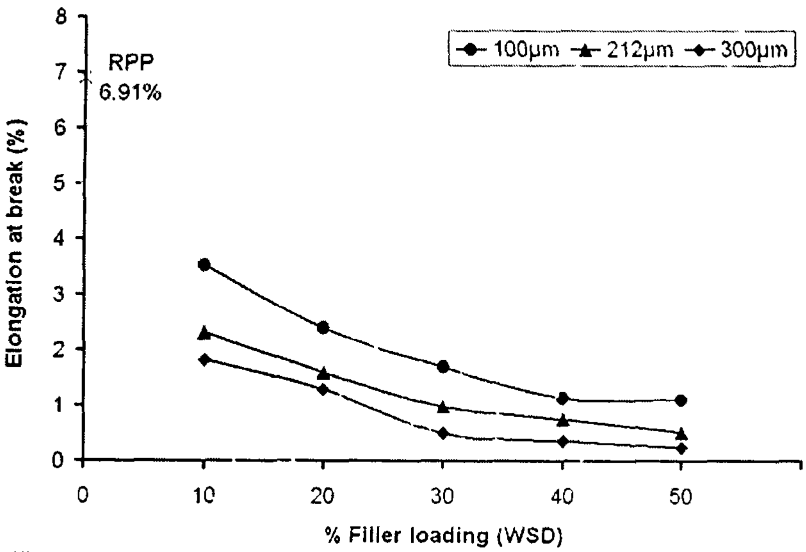

Figure 4. Effect of filler size and filler loading on elongation of WSD-RPP composites.

of 100 μm WSD, followed by 30% filler loading with strength of 14.98 MPa. Composites with 50% filler loading and particle size 300 μm displayed the lowest value tensile strength, dropped by 50% of the highest tensile strength value of 7.6 MPa.

Unlike tensile strength, the tensile modulus increased as filler loading increased from 10 to 40% (Figure 3). However, above 40%, the tensile modulus decreased as filler loading increased. The drop is due to poor compatibility of WSD and RPP matrix at high loading. WSD at high loading tends to form agglomerate, which caused poor

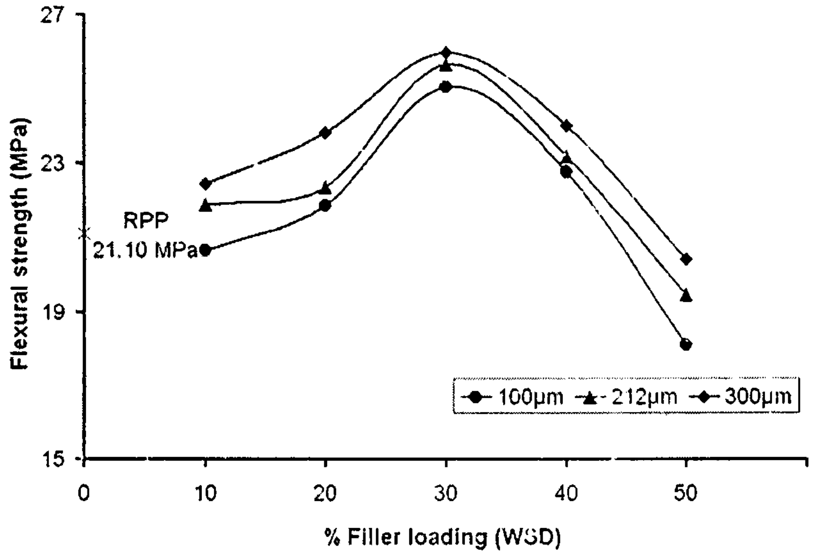

Figure 5. Effect of filler size and filler loading on flexural strength of WSD–RPP composites.

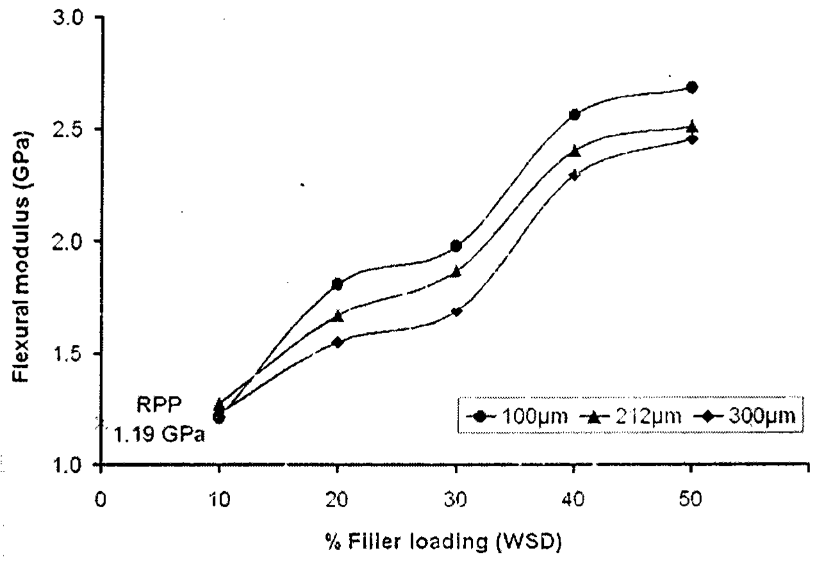

Figure 6. Effect of filler size and filler loading on flexural modulus of WSD–RPP composites.

incorporation between polar filler and nonpolar matrix. Thus, it has affected the stiffness of composites, because without modification, coupling agent or binder, the mixing between WSD and RPP is harder, primarily when the filler loading was raised. In general, we note that the increase of filler size has increased the tensile modulus of the composites. The lowest tensile modulus of 1.36 GPa was obtained from 50% filler loading of

300 µm WSD, followed by 212 (1.65 GPa) and 100 µm (1.74 GPa) of the same WSD loading [16].

Figure 4 shows the elongation of samples before break. It can be seen that, elongation at break of composites decreased proportionally to the increased percentage of WSD filling. It obviously proved that the reduction of RPP percentage has reduced the ductility and elongation of the composites. Also, the increase of WSD size has caused the composites to become more brittle with less elongation. As the size of the filler increased (212 and 300 µm), the elongation has decreased due to poor compatibility between WSD filler and RPP matrix [16,17]. Thus, the interfacial strength also reduced and caused the failure of composites with bigger filler size. As we can see, the highest percentage of elongation of 3.51% was obtained from 10% filler loading of 100 µm WSD whereas the lowest value, 0.24% (which is 3.27% less) was obtained from 50% filler loading of 300 µm WSD.

The flexural strength of samples were determined to measure the ability of composites to withstand bending forces applied perpendicular to its longitudinal axis or the maximum stress in the outer layer of the test specimen at rupture. Three point bending test was performed to study the effect of filler size and filler loading on flexural behavior.

Flexural strength increased with WSD loading up to 30%. However, beyond that point, the composites show reduced properties. This occurrence implied that the samples with higher WSD filling were unable to withstand higher stress. At this stage, the interactions between WSD and RPP matrix were very poor, where the amount of WSD filled did not sufficiently wet through with the matrix. Highest flexural stress was obtained at 30% filler loading for each filler size. The values are 25.96, 25.62, and 24.99 MPa for 300, 212, and 100 µm, respectively. There are only slight differences between these values, showing reduction of only 1 to 2% when using different size of WSD for the composites. Unlike tensile properties, 300 µm filler size showed the best fortifying capabilities as it shows highest flexure strength compared to the other sizes (212 and 100 µm). This may be attributed to bigger particle size (300 µm) that allowed better bonding, enhancing restraining between WSD and RPP when flexure stress is applied (Figure 5).

Flexural modulus was obtained from the load-deflection curves plotted during the test. In contrast with flexural strength, the trend for the modulus shows increase of value as the WSD size filled in composites increased as shown in Figure 6. It indicated that smaller particle size (100 µm) influence the stiffness of the composites and increased the modulus. The stiffness and modulus value also increased as the filler loading increased [10,16].

The toughness of composites shown in Figure 7. Toughness indicates energy gained of the composites before the failure. The increment of load filler percentage reduced the toughness because WSD has increased the stiffness of the composite which also lessen the toughness of composites. Composites with 10% filler loading displayed the highest toughness behavior for each size. The highest value, 0.23 J was obtained by 300 µm WSD, followed by 212 µm and the lowest was 100 µm, being 0.19 and 0.17 J respectively. The highest value of toughness of composites (0.23 J) is 77% higher than the toughness of RPP without filler loading (0.13 J). Composites with bigger filler size (300 µm) displayed better toughness compared to the smaller filler size (100 µm) This was due to better adhesion between bigger particle size of WSD and RPP matrix. Bigger particles provided larger area for the bonding.

Figure 8 shows result of impact strength of the composites. In general, the impact strength improved as filler size decreased. In this case, samples with smaller filler size (100 µm)

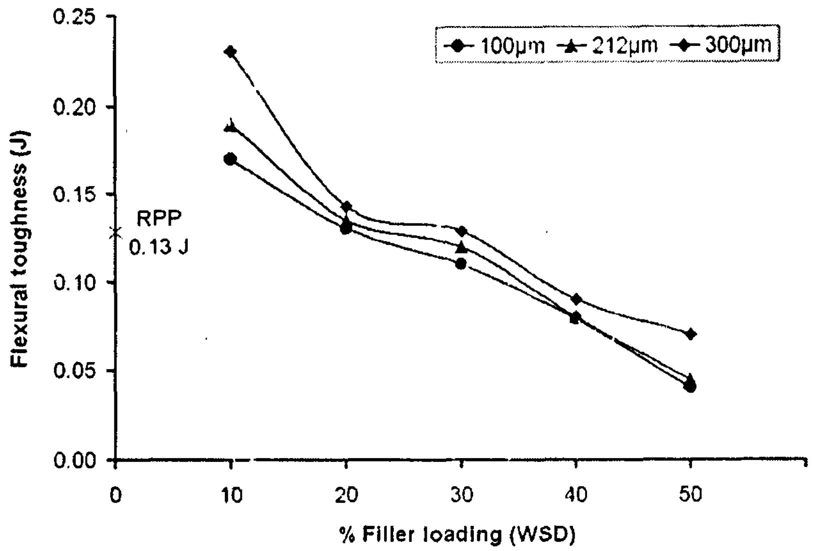

Figure 7. Effect of filler size and filler loading on flexural toughness of WSD–RPP composites.

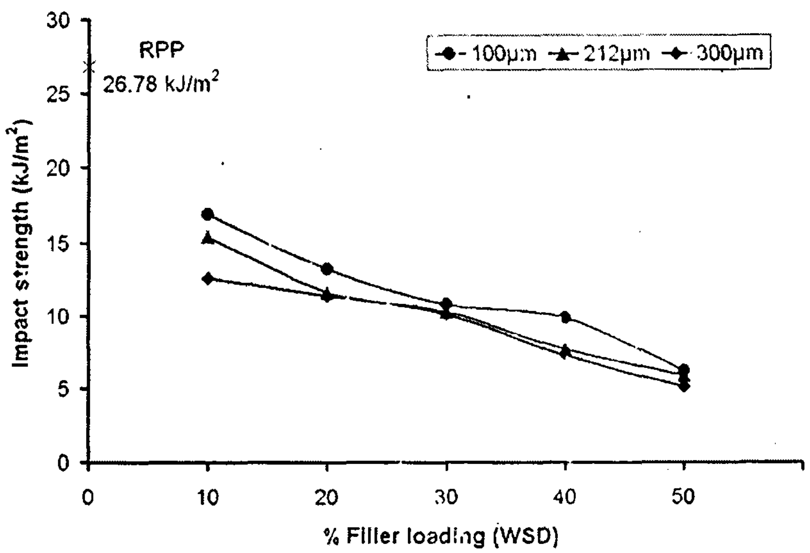

Figure 8. Effect of filler size and filler loading on flexural strength of WSD–RPP composites.

posed higher homogeneity and relatively higher absorption energy than larger ones (212 and 300 μm) of impact strength. This reflected the reduction of impact energy during crack formation and failure [16]. However, the impact strength decreased as filler loading increased. This was due to the stiffness increment which simultaneously reduced the impact strength as filler loading increased.

Figure 9 shows the SEM micrograph was taken on the impact surface failure. The results show that poor filler-matrix bonding between WSD filler and RPP matrix

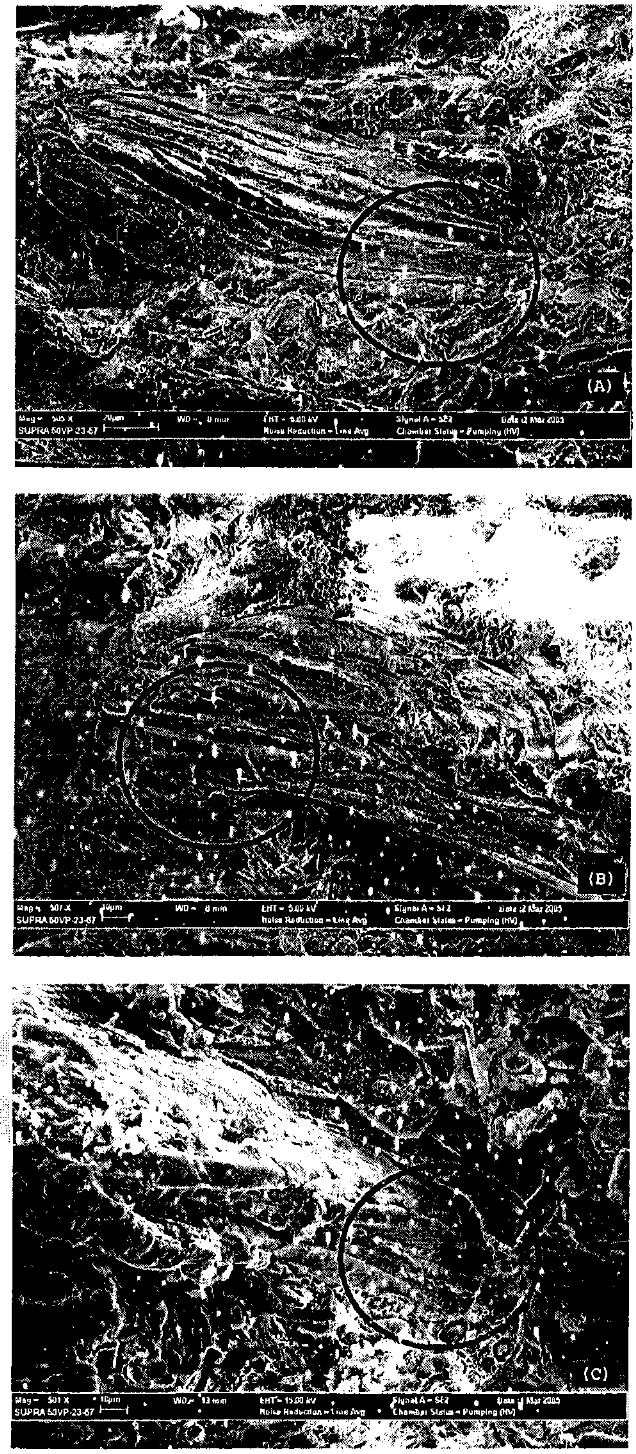

Figure 9. *SEM micrograph of impact fracture of filler-matrix bonding on (A) 100 μm & (B) 212 μm WSD filler (X 500), showing good filler-matrix bonding, fiber failure; and (C) 300 μm WSD filler (X 500) showing poor filler-matrix bonding.*

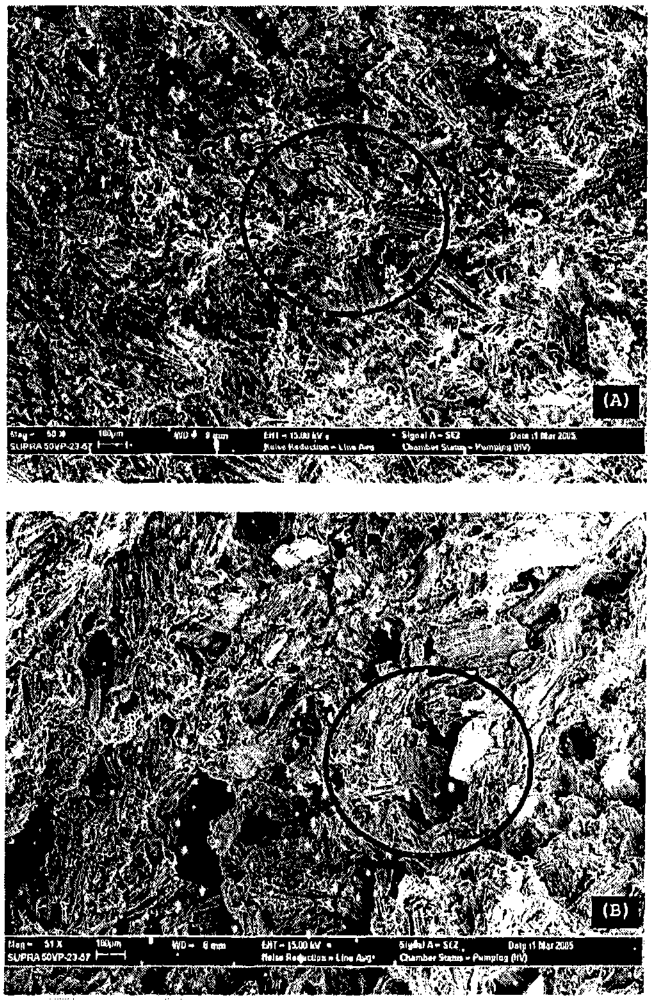

Figure 10. SEM micrograph of impact fracture of filler-matrix bonding on: (A) 30% WSD filler loading (X100), showing good filler-matrix bonding and (B) 50% WSD filler loading (X 100) showing poor filler-matrix bonding, many fiber pull-out.

as WSD filler size increased (up to 300 μm). Figure 9(A) and (B) shows the fracture of impact failure of 100 and 212 μm WSD filler loading, respectively. With comparison, 100 μm filler size WSD exhibited better filler-matrix bonding than 212 μm filler size. These figures also show that fiber failure, in some cases it seems to occur with rotation around the cell wall, following the microfibrilous structure. These would be expected to increase the energy absorbing properties of the composites. Hence, this phenomena reflects to high mechanical properties and low water absorption of composites. Figure 9(C) shows poor filler-matrix bonding of composites. The figure clearly shows that, initial crack tip of filler matrix bonding and short fiber pull-out. Figure 10(A) and (B) shows the SEM micrograph of failure surface of 30 and 50% filler loading in the order. We can see poor homogeneity of 50% filler loading with lots of voids as compared to 30% filler loading.

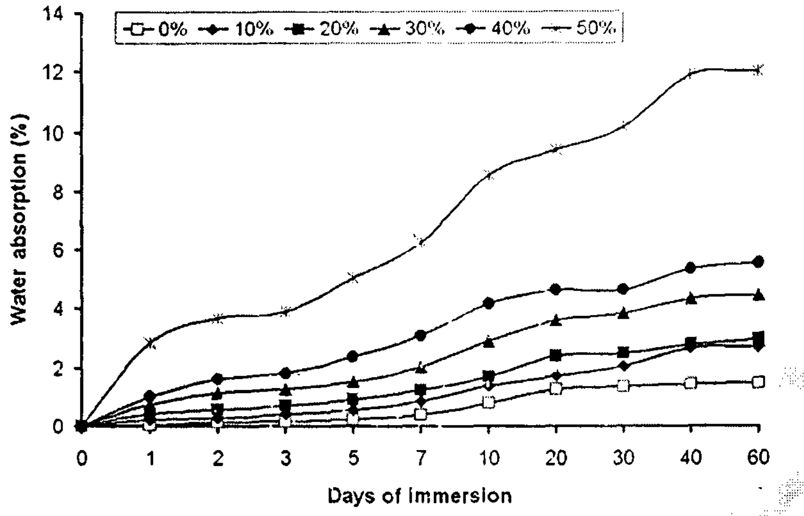

Figure 11. Effect of filler loading on water absorption of 100 μm WSD–RPP composites.

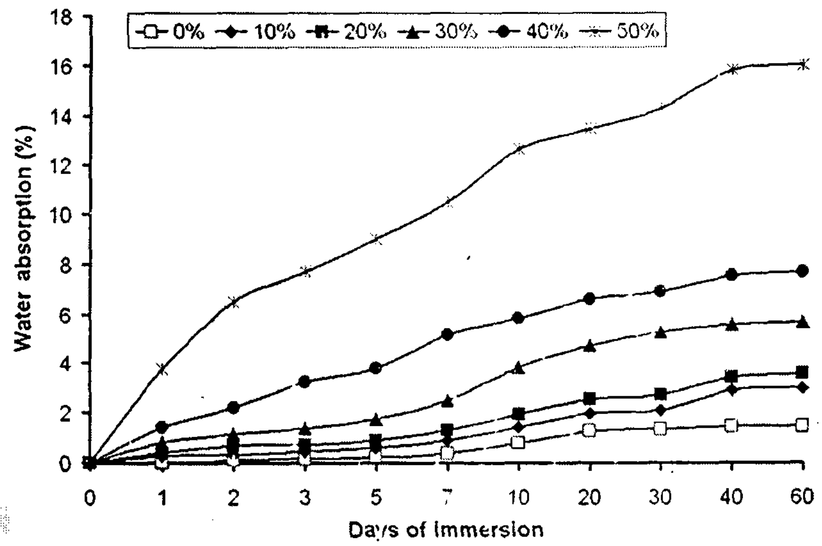

Figure 12. Effect of filler loading on water absorption of 212 μm WSD–RPP composites.

Figures 11–13 show water absorption properties of samples of each filler size composites. All the plots illustrate same trend, whereby water uptake of the composites increased as filler loading increased. This is because the more hydroxyl groups are available, the more water is absorbed. As we compare, the absorption also increased as the size of filler increased. Also, bigger particle size tends to absorb more water during the test. The interaction between filler-matrix bonding has altered hydrophilic nature of WSD and decreased the water uptake by the composites as compared to WSD [17].

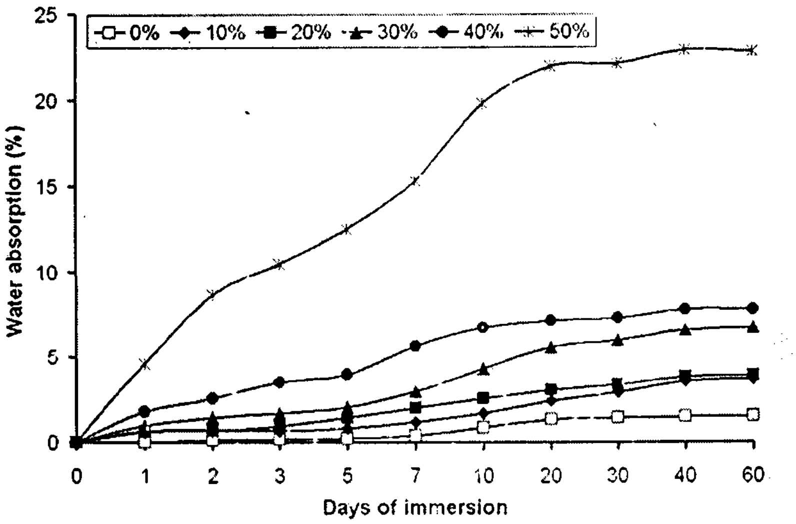

Figure 13. *Effect of filler loading on water absorption of 300 μm WSD-RPP composites.*

CONCLUSIONS

The conclusions from this study are summarized as follows:

1. In general, recycled polypropylene (RPP) filled wood saw dust (WSD) composites exhibited lower mechanical and water absorption properties than cast RPP alone.
2. Composites with smaller filler size (100 μm) displayed higher tensile and impact properties compared to the larger ones (212 and 300 μm). It is believed that better filler dispersion is the main factor responsible for the observed trends.
3. Increased filler loading, from 10 to 50% of WSD in RPP, displayed decreased tensile strength and impact properties, but increased flexural strength and modulus (except at 40% filler loading above).
4. The interaction between WSD and RPP has reduced the rate of water absorption of the composites. Water uptake increased as WSD size and loading increased.

ACKNOWLEDGMENTS

The authors would like to thank the Ministry of Science, Technology and Environment (Malaysia) and Universiti Sains Malaysia, Penang for offer of IRPA grant that has made this research work possible.

REFERENCES

1. Kryzysik, A. M., Youngquist, J. A., Myers, G. E., Chahyadi, I. S. and Kolosick, P. C. (1991). Wood-polymer Bonding in Extruded and Non-woven Composite Panels, *Journal of Applied Polymer Science*, **78**: 1685–1697.
2. Gilbert, J. M., Samuel, S. O., Gerald, D. S., Leonard, S. M. and Van Nostrand (1974). *SPI Handbook of Technology and Engineering of Reinforced Plastics/Composites*, **2nd edn**, pp. 319–323, Reinhold Company.

3. Donna, A. J., David, A. J., James, L. U., Roger, M. R., Rodney, J. and Daniel, J. (1999). Weathering Characteristics of Fiber/Polymer Composites, In: *Proceedings of 5th International Conference on Woodfiber-Plastic Composites*, Forest Products Society, pp. 203–209.
4. Youngquist, J. A. (1995). Unlikely Partners? The Marriage of Wood and Nonwood Materials, *Forest Products Journal*, **45**(10): 25–30.
5. Abdul Khalil, H. P. S., Ismail, H., Rozman, H. D. and Ahmad, M. N. (2001). The Effect of Acetylation on Interfacial Shear Strength between Plant Fibres and Various Matrices, *European Polymer Journal*, **37**: 1037–1045.
6. Abdul Khalil, H. P. S., Ismail, H., Ahmad, M. N., Ariffin, A. and Hassan, K. (2001). The Effect of Various Anhydride Modification on Mechanical and Water Absorption Properties of Oil Palm Empty Fruit Bunches Reinforced Polyester Composites, *Polymer International*, **50**: 1–8.
7. Matsuda, H. (1993). Preparation and Utilization of Esterified Woods Bearing Carboxyl Groups, *Wood Science Technology*, **27**: 23.
8. Bledzki, A. K. and Gassan, J. (1999). Composites Reinforced with Cellulose Fibres, *Prog. Polymer Sci.*, **24**: 221–274.
9. Oksman, K., Wallstóm, L., Berglund, L. A. and Filho, R. D. T. (2002). Morphology and Mechanical Properties of Unidirectional Sisal-epoxy Composites, *Journal of Applied Polymer Science*, **84**: 2358–2365.
10. Hanafi, I., Jaffri, R. M. and Rozman, H. D. (2003). The Effects of Filler Loading and Vulcanisation System on Properties of Oil Palm Wood Flour-natural Rubber Composites, *Journal of Elastomers and Plastics*, 35(2): 181–192.
11. Ishak, Mohd. Z. A., Yow, B. N., Ng, B. L., Abdul Khalil, H. P. S., Rozman, H. D. (2001). Hygrothermal Aging and Tensile Behavior of Injection Molded Rice Husk filled Polypropylene Composites, *Journal of Applied Polymer Science*, **81**: 742–753.
12. Welling, M. S. (1979). The Recycling of Thermoplastic Wastes, *Recycling of Thermoplastic Wastes*, Verein Deutscher Ingeniure, Germany, pp. 1–7.
13. Miles, D. C. and Briston, J. H. (1996). Polymer Technology, *Thermoplastics: Polyolefins*, 3rd edn, pp. 225–229, Chemical Publishing Co.
14. Carruthers, S. P. (1994). Fibres, In: Carruthers, S. P., Miller, F. A. and Vaughan, C. M. A. (eds), *Crops for Industry and Energy*, Report of a Study Sponsored by the Ernest Cook Trust, CAS Report, **15**: 93–108.
15. ASTM (1999). Standard Methods of Evaluating the Properties of Wood-based Fibre and Particle Panel Materials. ASTM D-1037–99: American Society for Testing and Materials, Philadelphia, PA.
16. Ismail, H., Nizam, J. M. and Abdul Khalil, H. P. S. (2001). The Effect of a Compatibilizer on the Mechanical Properties and Mass Swell of White Rice Husk Ash Filled Natural Rubber/Linear Low Density Polyethylene Blends, *Polymer Testing*, **20**: 125–133.
17. Shahnaz, S. B., Abdul Khalil, H. P. S. and Maran, Mani R., (2003). The Effect of Anhydride Modifications on Mechanical Properties and Water Absorption of Recycled Polypropylene-wood Saw Dust Composites, In: *Proceeding of 17th Symposium of Malaysian Chemical Engineers (SOMCHE 2003)*, pp. 898–903, Penang.

Comparative study of the load ratings of wood filler and oil-palm fiber composite pallets using FEA analysis

Khoo, T.S.[1], Ratnam, M.M.[2] and Abdul Khalil, H.P.S.[3]

[1,2]*School of Mechanical Engineering, Engineering Campus, Universiti Sains Malaysia, 14300 Nibong Tebal, Penang, Malaysia.*
[3]*School of Industrial Technology, Universiti Sains Malaysia, 14300 Nibong Tebal, Penang, Malaysia.*
e-mail: [1]tensin04@yahoo.com, [2]mmaran@eng.usm.my
e-mail: [3]akhalil@usm.my

Abstract
The load rating and structural strengths of the material handling pallets made from wood fillers and oil-palm fiber composites were studied using computer modeling and finite element analysis. A conventional stringer-class pallet was modeled using Solidworks modeler and analyzed under support and load conditions known as 'stacked one unit load high'. The mechanical and physical properties such as ultimate tensile strength tensile modulus and density of the wood fillers and oil-palm fiber composites were used as an input into the analysis. Pallets made from wood fillers, oil-palm composites, as well as the polypropylene alone were used in the study. The comparative study has shown that oil-palm-ABS composite pallet has the highest load rating of 3281 kg and a maximum deflection of 6.19 mm.

Introduction

Promising technology is evolving for using waste or low grade wood component with polyolefin plastic (polypropylene) to make an array of high performance reinforced composite products (Krzysik *et al.*, 1991). The utilization of fillers from various sources into polypropylene (PP) has been an accepted route to achieve enhancement in material properties or cost saving possibilities. These fillers can be categorized as inorganic (such as carbon black, silica, calcium carbonate and talc) and organic. Calcium carbonate and talc are traditionally used fillers in most plastic industry (Hattotuwa *et al.*, 2002). However, organic fillers have become a strong competitor to inorganic fillers during the past few years. This may be due to their low densities, low cost, high durability and biodegradability (Bledzki *et al.*, 1999; Bledzki *et al.*, 2001; Oksman *et al.*, 2002; Hattotuwa *et al.*, 2002).

In recent years, use of fibers and powders derived from agricultural sources (such as sisal fiber and oil palm empty fruit bunch) has become a subject of interest in polymer composites, mainly due to the aforementioned advantages. Besides the improvement in the mechanical properties of the composites, environmental concern is believed to be one of the driving forces behind the use of natural fiber (Bledzki *et al.*, 1999; Bledzki *et al.*, 2001; Oksman *et al.*, 2002). Potential products made of natural fiber-reinforced composites (NFRC) include automobile and truck component and packaging application like containers, cartons and pallets. However, most of the existing products were restricted to low-load or load-free applications. Indeed, natural fiber reinforced composites have great potential for use in load bearing applications for the material handling pallets, crates, boxes, etc. Currently, nearly 400 millions wood pallets are produced annually, accounting for 86 percent of all pallets sold (McCoy, 2003). Most pallets are made from wood mainly because wood is cheap and easily available. Wood pallets, however, could undergo degradation due to environment factors such as heat, moisture and fungus attack especially when used in open space. Although NFRC pallets could also undergo degradation due to an attack by micro-organisms, the resistance to microbiological degradation can be improved by means of chemical modification (Hill *et al.*, 2001). This material, therefore, has significant potential for use as raw material in the fabrication of pallets especially due to the large quantity of agricultural waste fibers and fillers available, and the need to recycle plastic products.

The advantage of using computer for designing and analyzing (Qiao *et al.*, 1998; Wu *et al.*, 2003; Lim *et al.*, 2003) the pallets is that several designs can be modeled and tested theoretically to determine their load ratings before the actual product is fabricated, hence reducing overall cost and time involved in the fabrication of the actual prototype.

This work presents the modeling and finite element analyses (FEA) of natural fiber-reinforced composite pallets made from oil palm, wood fillers and recycled polypropylene in order to investigate their load ratings. Load ratings of several composites were carried out under support condition 'stacked one unit load high' and the results were then compared with load rating of polypropylene pallet.

Modeling and FEA

A stringer-class pallet, namely pallet model_1 (see Fig.1) with dimensions 1200mm(L) × 1000mm(W) × 100mm (H) was created using *Solidworks* modeler. This model was used in FEA software, *Cosmos/works* to determine its load ratings. Four materials were specified in separate runs:

Analysis 1: 40% wood flour-60% PP composites;
Analysis 2: coarse wood sawdust-PP composites;
Analysis 3: oil palm empty fruit bunch fibers-ABS (Acrylonitrile-Butadiene-Styrene) composites;
Analysis 4: recycled PP plastic;

All the mechanical properties of the natural fiber-reinforced composites were determined from previous work (Lim *et al.*, 2003; Shanaz *et al.*, 2003) and are shown in Table 1. Loading and support condition, stacked one unit load high (see Fig.2) simulates a situation where pallets are put in warehouse storage or shipping and the concrete floor supports the lowest pallet in the stack. Due to this reason, the bottom deck boards of the pallets were defined as fixed in the FEA analysis. A factor of safety (F.O.S) of 1.5 is justifiable for this support condition of stacked one unit load high in order to avoid over designing and premature failure during loading (Dieter, 1976). Since the load was applied uniformly on top deck boards of the pallets, the effective pressure could be calculated for given area, A using the following equation:

$$P = \frac{F}{A} \tag{1}$$

where P is the effective pressure and F is the force acting on the area. The maximum loads of each pallet under stacked one unit load high are tabulated in Table 2. The weights and strength-to-weight ratio are also given in Table 2.

Table 1 The mechanical and physical properties of natural fiber-reinforced composite materials.

Material Property	OPFRC (OPF-ABS)	WFRC (wood filler -PP)	Coarse wood sawdust-PP	PP only
Ultimate Tensile Strength, (MPa)	21.740	13.302	20.500	12.000
Modulus of Elasticity, (GPa)	2.410	1.171	1.510	1.150
Poisson Ratio	0.30	0.30	-----	-----
Density, (kg/m^3)	830	1042	1040	1145

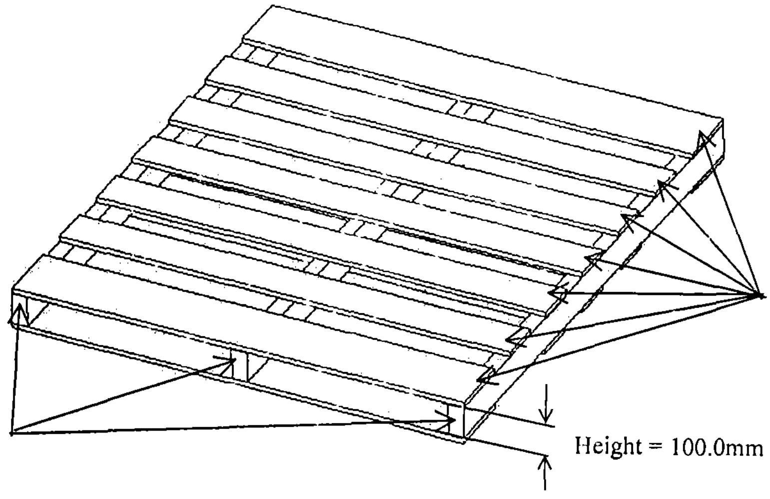

Fig.1 Solid model of stringer-class pallet.

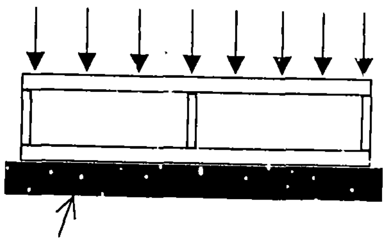

Fig. 2 Support and load condition of pallet for stacked one unit load high.

Results and discussion

From the results of analyses shown in Table 3 under support condition 'stacked one unit load high', the oil-palm fiber-ABS composite pallet was found to have the highest load rating of 3281.5kg and the lowest maximum deflection of 6.190mm under this maximum load. The smaller maximum deflection of oil-palm fiber-ABS composite pallet compared to other materials is due to the higher modulus of elasticity. The load rating of coarse wood sawdust-PP composite pallet and wood flour-PP composite were found to be 3104.5kg and 2022.2kg respectively. Comparisons of the load ratings of coarse wood sawdust-PP composite pallet and wood flour-PP composite pallet shows that the strength of fiber-reinforced composite depends considerably on the fiber-matrix interface. A well formed interface allows stress to transfer from the matrix to the fiber, and thus increasing the strength of material. The load rating of polypropylene pallet was found to be 1805.1kg showing that the reinforcement using fillers increases the strength more than 3 times in the case of oil-palm-ABS composite.

For the support condition 'stacked one unit load high', the deflection under maximum load is an important parameter that determines failure of a pallet because the thickness of a standard pallet jack fork is 83 0mm and, thus deflection that causes the gap between the upper and lower deckboards to reduce to below 83.0 mm is not acceptable, i.e. a deflection of more than 19.0 mm is not allowed.

Results in Table 3 also show that oil-palm fiber-ABS composite pallet is the most lightweight pallet (28.12 kg) whereas pallet made from polypropylene alone has the highest weight. Comparison of load capacity-to-weight ratio shows that pallets made from oil-palm-ABS composite have the highest value, followed by wood based-PP composite and polypropylene pallets. These results reveal that the obvious advantage of using natural fiber-reinforced composites (either in powder or fiber form) in the manufacture of materials handling pallets.

Table 2 maximum deflections, load capabilities, weights and load-to-weight ratios of pallets made from different materials.

Material	Load, kg	Maximum deflection, mm	Weight, kg	Load-to-weight ratio, kg/kg
Oil-palm fiber-ABS	3281.5	6.190	28.12	116.70
Wood flour-PP	2022.2	7.853	35.30	57.30
Coarse wood sawdust-PP	3104.5	9.335	35.24	88.10
PP only	1805.1	7.254	38.79	46.50

Conclusions

FEA analyses results showed that oil-palm fiber-ABS composite pallet has the highest load capacity compared to pallets made from the other materials investigated. In addition, oil-palm-ABS composite pallet has the highest load-to-weight ratio. However, in comparison of cost, wood based-polypropylene composite becomes another alternative since this composite can be made without undergoing complicated and costly manufacturing process. Besides, reformability and moderate load rating of this composite material are another advantages compared to oil-palm-ABS composite.

References

1. Bledzki, A.K. and Gassan, J., 1999, *Composites reinforced with cellulose based fibers*, Prog.Polym.Sci., 24:221-274
2. Bledzki, A.K., Zhang, W. and Chate, A., 2001, *Natural fiber-reinforced polyurethane microfoams*, Composite Science and Technology, 61:2405-2411
3. Dieter, G.R., 1976, *Mechanical fundamental: Mechanical Metallurgy*, McGraw-Hill, New York
4. Hill, C.A.S. and Abdul Khalil, H.P.S., 2001, *The effect of fiber treatments upon the mechanical properties of coir or oil palm fiber reinforced polyester composites*, Journal of Applied Polymer Science, 78: 1685-1697
5. Krzysik, A.M., Youngquist, J.A., Myers, G.E., Chahyadi, I.S. and Kolosick, P.C., 1991, *Wood-polymer bonding in extruded and non-woven web composite panels*, Forest Products Research Society, 183-189
6. Lim, J.H., Ratnam, M.M. and Abdul Khalil, H.P.S., 2003, *An experimental and finite element analysis of the static deformation of natural fiber reinforced-composite beam,* Polymer Testing, 22: 169-177
7. McCoy, M., 2003, *Pallets that make the extra trip*, Modern Material Handling
8. Oksman, K., Wallstőm, L., Berglund, L.A. and Filho, R.D.T., 2002, *Morphology and mechanical properties of unidirectional sisal-epoxy composites*, Journal of Applied Polymer Science, 84: 2358-2365
9. Qiao, P. Davalos, J.F. and Zipfel, M.G., 1998, *Modeling and optimal design of composite-reinforced wood railroad crosstie*, Composite Structures, 41: 87-96
10. Shanaz, S.B., Abdul Khalil, H.P.S., Ratnam M.M., May 2003, Recycled polypropylene (PP)-wood sawdust composites: The effect of acetylation on mechanical and water absorption properties, Advanced Technology Congress, Putra Jaya, Malaysia.
11. Wu, H.C., Mu, B. and Warnemuende, K., 2003, *Failure analysis of FRP sandwich bus panels by finite element method*, Composite Part B, 34: 51-58

CHAPTER 5

FASTENING STUDY

5.0 Introduction

In structures composed of polymer matrix composite materials, components must be joined such that overall structure retains its structural integrity while it is performing its intended function (Vinson, 1989). According to Stokes (1989), joining of plastic and plastic composites is becoming important for several reasons. First, such materials are increasingly being used in complex structural assemblies, in which joining considerations and cost are becoming important. Besides, the emerging structural (load bearing) applications of polymeric materials require structural joints that must withstand static and fatigue loads. Joining metallic structures is a mature technology involving riveting, bolting, welding, glueing, brazing, soldering and other methods. However, for most polymer matrix composites only mechanical fastening and adhesive bonding can be utilized (Vinson, 1989; Stokes, 1989).

A mechanical connection consists of two or more members joined together with one or more fasteners. Mechanical connections are important because they provide continuity to the joined members and strength and stability to the system (Committee of ASCE, 1997). Mechanical fastening can either be permanent, or consist of joints that can be fastened and unfastened. Snap fits, screws (includes bolts and nuts) and metal inserts are used to provide operable joints while rivets are examples of methods used for achieving permanent joints (Stokes, 1989; Spotts and Shoup, 1998). However, this chapter focuses only on mechanical fasteners used in the assembly of the pallet. According to Mackerle (2003), fasteners are immensely important in the assembly of machine, furniture, pallets, automobile, etc. As links for interacting parts, they are used to transmit forces created by a load to the joined parts. The advantage of mechanical fasteners is that, despite their design simplicity, they provide a high clamping force and ease of disassembly for maintenance. Mechanical fasteners, therefore, have been used almost worldwide since the 14^{th} century (Sase *et al.*, 1998).

Selection of a fastener for a specific design application depends on the type of connection and the required strength. Each connection must be designed to transmit forces adequately and provide satisfactory performance for the life of the structure without causing splitting, cracking or excessive deformation of the joint members (Committee of ASCE, 1997).

The main objective of this part of the research is to find a suitable fastening method, mechanical fastener types and sizes for used in assembly of the stringer-class natural filler composite pallet shown in Figure 5.1. In order to achieve the above objective, the following sub-objectives were identified:

1) To investigate the ease of fastening the screws to the composite materials with and without pre-drilling process.
2) To investigate the minimum depth to which the guide hole needs to be drilled in order to enable various screw sizes (#3 to #10) to penetrate into the composite easily.
3) To compare the ease of fastening the composite material using different screw types, namely woodscrews and tapping screws.
4) To determine the minimum distance between two screws, minimum edge distance and minimum end distance of screws to the members in order to assemble the parts without cracking.
5) To compare the ease of fastening for different compositions of composite materials with increasing filler contents.

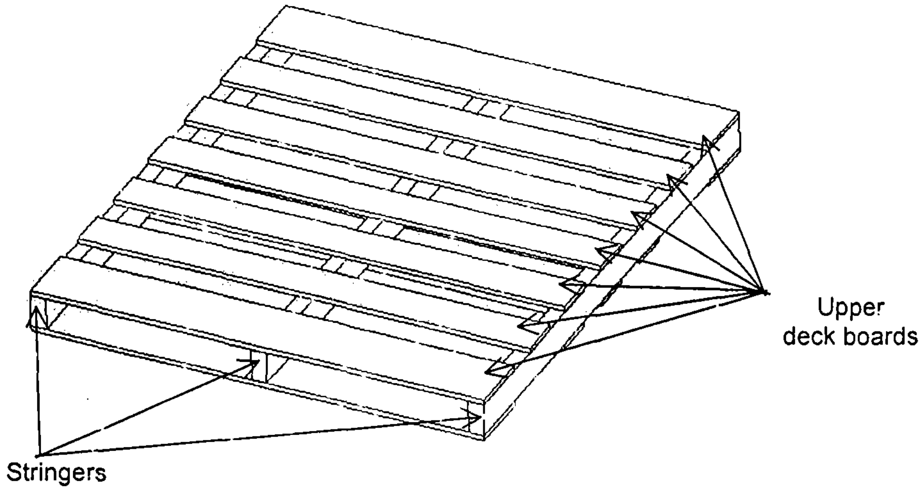

Figure 5.1: Solid model of stringer-class pallet.

5.1 Screw Terminology

A screw thread is a ridge of uniform section in the form of a helix on the internal or external surface of a cylinder (Figure 5.2). External threads are screw threads on bolts, woodscrews and studs while internal threads are referred to nuts and tapped holes (Blake, 1986). The screw threads have capability to develop and transfer tremendous forces when properly assembled. With this reason, some basic knowledge about screw threads such as the thread profile and screw terminology is necessary.

Figure 5.2 shows that the thread profile is made up of crest, root and flanks where the flanks join between root and crest. Besides, Figure 5.2 also shows the terminology of the screw threads as follow: *pitch*, *p* is the distance measured parallel to the thread axis between adjacent threads. Unified threads are designated in *number of threads forms per inch*, *N*. An important relationship between pitch and threads per inch (TPI) is:

$$p = \frac{1}{N} \tag{5.1}$$

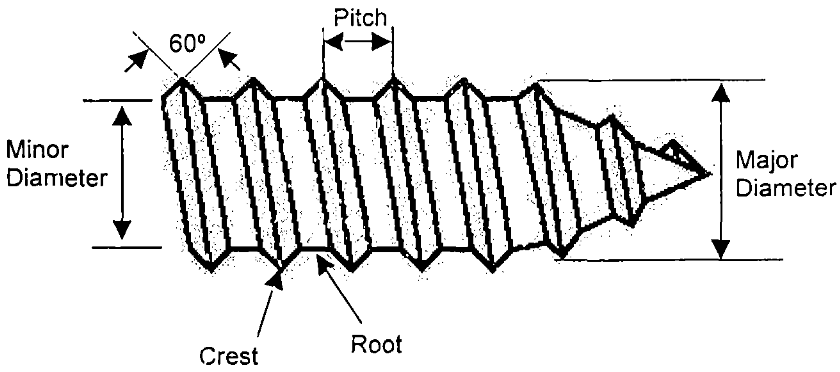

Figure 5.2: Typical spaced threads (Resource: http://www.jglen.com, 2000).

The *major diameter*, *D* is the largest diameter of a screw thread while the *minor diameter*, *d* is the smallest diameter of screw thread (Blake, 1986). The major diameter can be measured with a simple caliper or slot gauge accurately enough to determine its nominal diameter. The measurement of *major diameter* is taken on the crest. Besides, the *minor diameter* requires specialist measuring equipment for technical accuracy. The thread profile for woodscrews and tapping screws are named as spaced threads profile. These screws are designed to form their own thread especially on a pre-drilled hole. The diameter of imperial spaced threads can be expressed as gauge number or nominal size, # (http://www.jglen.com, 2000). An example given in training manual by *James Glen Pty Ltd* (2000) shows that a standard tapping screw of size #6-20 is defined where 6 is the gauge number (equivalent to 0.138 inches) and 20 refers to the threads per inch of the tapping screws. For metric spaced threads, however, unlike Unified threads, the imperial designations of the above tapping screw, is given as M6-1.27, where prefix 'M' represents the metric system, 6 is thread with nominal major diameter of 6 mm while the threads per inch (TPI) is represented in form of thread pitch, *p* which is 1.27 mm (equivalent to 0.05 inch).

5.1.1 Wood Screws

Wood screws are normally used as fasteners in the assembly of wood structures. Nowadays, the manufacture of all wood screws must comply with American National Standards Institute/American Society of Mechanical Engineers' (ANSI/ASME) Standard B18.6.1 (Kent, 1950). The wood screws are thread forming screws and are generally available in three types, such as flat, oval or round heads (Figure 5.3). The flat head screw is most commonly used if a flush surface is desired. The principal parts of a screw are the head, shank, thread and core (Figure 5.3). The root diameter for most sizes of screws averages about two-thirds the shank diameter and wood screws must be threaded along at least two-thirds of their length. Wood screws are usually made of steel, brass or alloys and may have specific coating such as nickel, chromium or cadmium. The wood screws are classified according to material, type, finish, shape of head and diameter (gauge of the shank). Several dimensions of American Standard Wood Screws which were used in this study are given in Table 1 (Kent, 1950). The terms of a typical flat head woodscrew such as nead diameter, width of slot, depth of slot, etc which are illustrated in Table 5.1 are illustrated in Figure 5.4.

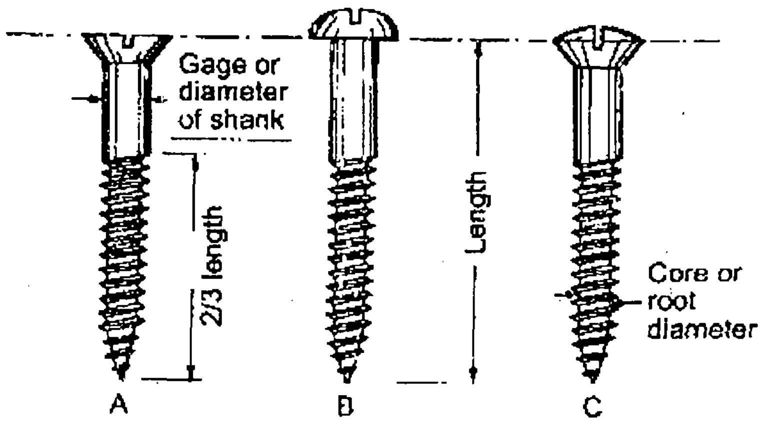

Figure 5.3: Common types of wood screws: (A) Flat head; (B) Round head; and (C) Oval head (Resource: Kent, 1950).

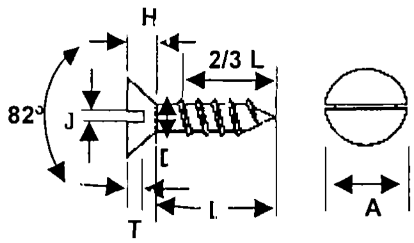

Figure 5.4: Typical flat head woodscrew with designated symbols (Resource: Kent, 1950).

Table 5.1: Several dimensions of American Standard Wood Screws (ASA B18.6-1947, all dimensions are in inches) (Resource: Kent, 1950).

Nominal size, #	Diameter, D	Threads per inch	Flat head			
			Head Diameter, max, A	Height of Head, max, H	Width of slot, min, J	Depth of slot, T Flat head, min
3	0.099	24	0.199	0.059	0.027	0.017
4	0.112	22	0.225	0.067	0.031	0.020
5	0.125	20	0.252	0.075	0.036	0.022
6	0.138	18	0.279	0.083	0.039	0.024
8	0.164	15	0.332	0.100	0.045	0.029
9	0.177	14	0.358	0.108	0.045	0.032
10	0.190	13	0.385	0.116	0.050	0.034

5.1.2 Tapping Screws

Current trends in fastenings of wood or composite materials also include the tapping screw (Figure 5.5). Tapping screws, also known as sheet metal screws, have threads the full length of the shank and may have some advantages for certain specific applications. For instance, they are heat treated and hardened and may be used in applications that required more corrosion resistance. Besides, they can be used in aluminum castings, plywood, soft and high impact plastics. There are various types of tapping screws in the market, namely type 'A', type 'AB', type 'B' and type 'BP'. Only two of them, type 'A' and 'AB' tapping screws have a fairly sharp point, known as gimlet point which is suitable to be used in fastening with small pilot hole on the materials while the others have flat tip. Several dimensions of type 'A' tapping screw which were used in this study can be referred to ANSI Standards B18.6.4-1998 (http://www.smithfast.com, 2000).

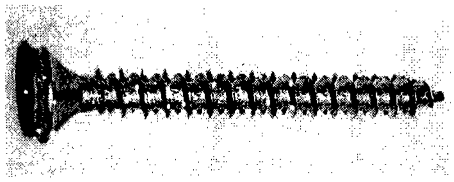

Figure 5.5: Type 'A' countersink tapping screw.

5.2 Comparison of Thread Series

The current Unified Coarse thread series (UNC) is patterned on the thread series introduced by Whitworth in the mid-19th century. Over years, as production capabilities improved, many special purpose thread series were developed. For fasteners, there are four common thread series, namely (i) Unified Coarse (UNC), (ii) Unified Fine (UNF), (iii) 8-thread (8UN) and (iv) Metric Coarse (M). According to Blake (1986), fine threads are better for tapping thin walled members. Fine threads are also easier to tap in hard materials since less metal is being removed. On the other hand, coarse threads are better for tapping brittle material, which tend to crumble such as the composite materials. Besides, coarse threads can tolerate more abuse during handling and can be easier to assemble and disassemble while fine threads provide better adjustment accuracy because of their smaller helix angles and require less torque to develop a given tension. In other words, use of coarse or fine thread series fasteners depends more on the physical property of the materials and their purpose of applications. Coarse threads are used in the fastening study due to its ease in tapping brittle material and are easier to fasten and unfasten compared to fine threads series.

5.3 Methodology

5.3.1 Preparation of Test Specimens for Fastening Study

Two molds were used to prepare the test specimens used in the fastening study as shown in Figure 5.6. The thicker mold was used to prepare specimens assumed as deck board while the other mold was used to prepare the stringer. The raw materials, comprising of wood filler and crushed recycled plastic were poured into the mold and hot-pressed in a hot-press machine under 190°C for 20 min at 8MPa. The molds were then cold pressed inside the machine with power switched off for 24 hours in order to allow homogenous boards to be formed. These boards were then cut into the dimensions of 100mm (L) × 50mm (W) × 15mm (T) and 40mm (L) × 40mm (W) × 50mm (T) respectively. Figure 5.7 shows the hot-pressed boards before cutting while Figure 5.8 shows of the test specimens after cutting to their dimensions.

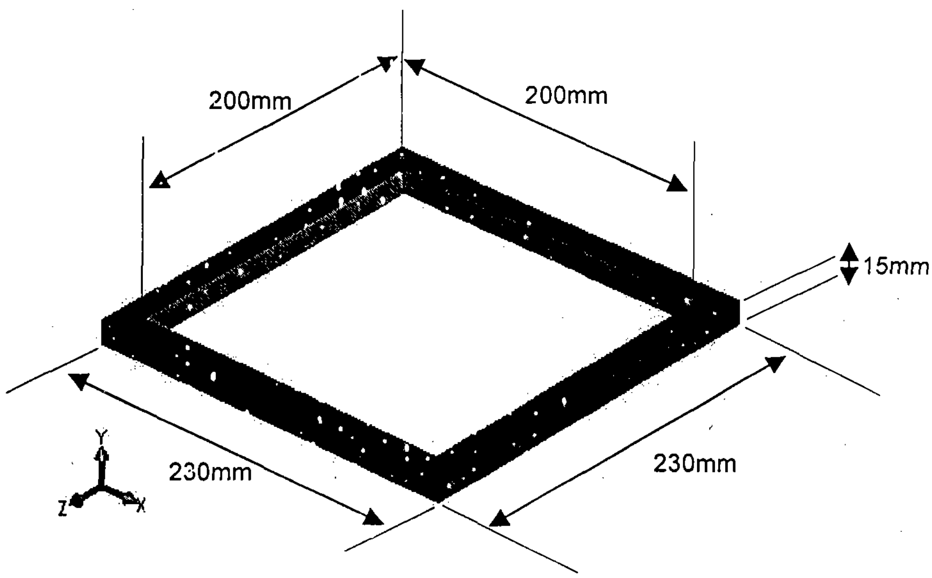

(a)

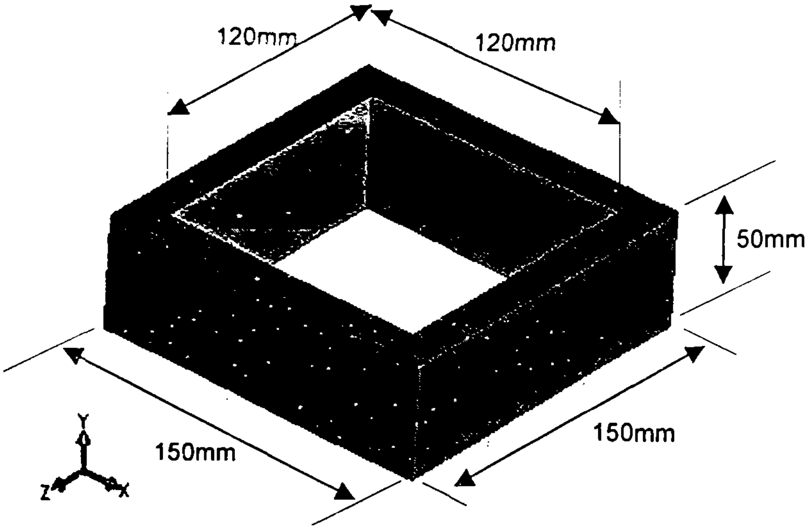

(b)

Figure 5.6: Molds used for preparing test specimens (a) deck boards, (b) stringers used in fastening study.

Four different combinations of reinforced composites of wood fillers and recycled plastic were used, with increase of wood fillers content in steps of 10% to 40%. Since the most suitable fastening method will be later applied to the full size pallet, the thickness of the actual pallet size was used during forming of the test specimens for the fastening study. The assembly of the deck board to the stringer of a pallet model is shown in Figure 5.9. The other unrelated dimensions such as length and width of the specimens were scaled down with the condition that they still have sufficient space for edge distance, end distance and spacing between two screws. This saves material required in fabrication of the test specimens. Woodscrews and tapping screws of nominal size from #3 (2.5146mm) to #10 (4.8260mm), (except screws of size #7 (3.835mm)) were used for fastening the various members of the scaled down and full size pallet model. It was not possible to obtain size #7 screw from local suppliers.

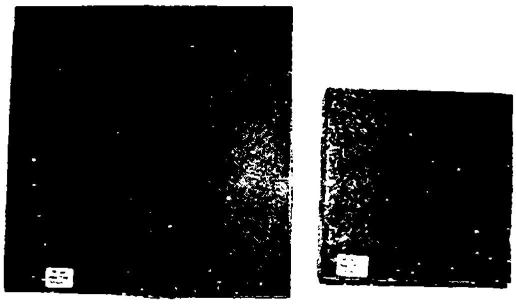

Figure 5.7: Top view of boards used in the fastening study.

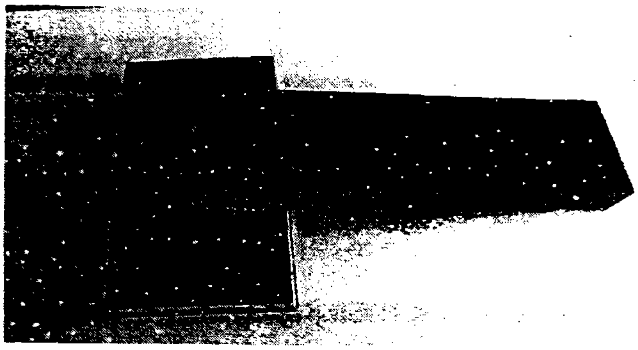

Figure 5.8: Image of the test specimens used in fastening study after cutting.

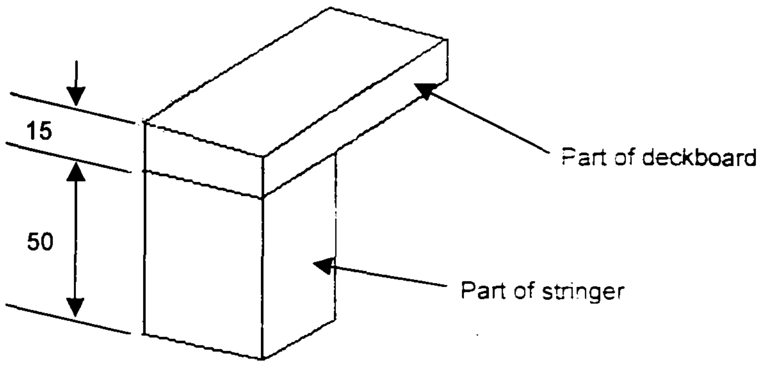

Figure 5.9: The actual thickness of the fastening members which simulates and assembly of full size pallet (All dimensions are in millimeters).

5.3.2 Fastening Study of Wood Fillers-Polypropylene Composites

A cordless driver tool, ('NICEMAN®' model NM600) shown in Figure 5.10 was used to fasten the screws into the composite material in the fastening study. Before the start of fastening study, two important factors that need to be considered are (i) clamping of the work piece and (ii) selection of an appropriate torque setting of the cordless driver tool. All the work pieces were set up properly and fastened securely before performing the drilling or driving operation, especially when drills up to 9.5 mm in diameter were used (Krar and Oswalds, 1977).

An appropriate torque setting of the cordless driver tool was required to prevent driving the screw too deep or prevent damage to the tool. Too low torque value can result in unnecessary wear of fasteners as well as the parts being secured. If insufficient pressure is applied to the fasteners, uneven loads will be transmitted throughout the assembly which may result in excessive wear or premature failure. High torque value can be equally damaging because of failure of screw from over-stressing. Besides, the torque setting of the tool also depends on the type and size of the screws and materials used in the application (cordless driver tool user guide, 2002). There are 15 torque settings on the cordless driver tool used in this research, which the torque value can be adjusted using the torque adjusting knob shown in Figure 5.10. The torque setting on the drill was adjusted to the lowest value of '1' during fastening study in order to prevent damage of the test specimens caused by high torque.

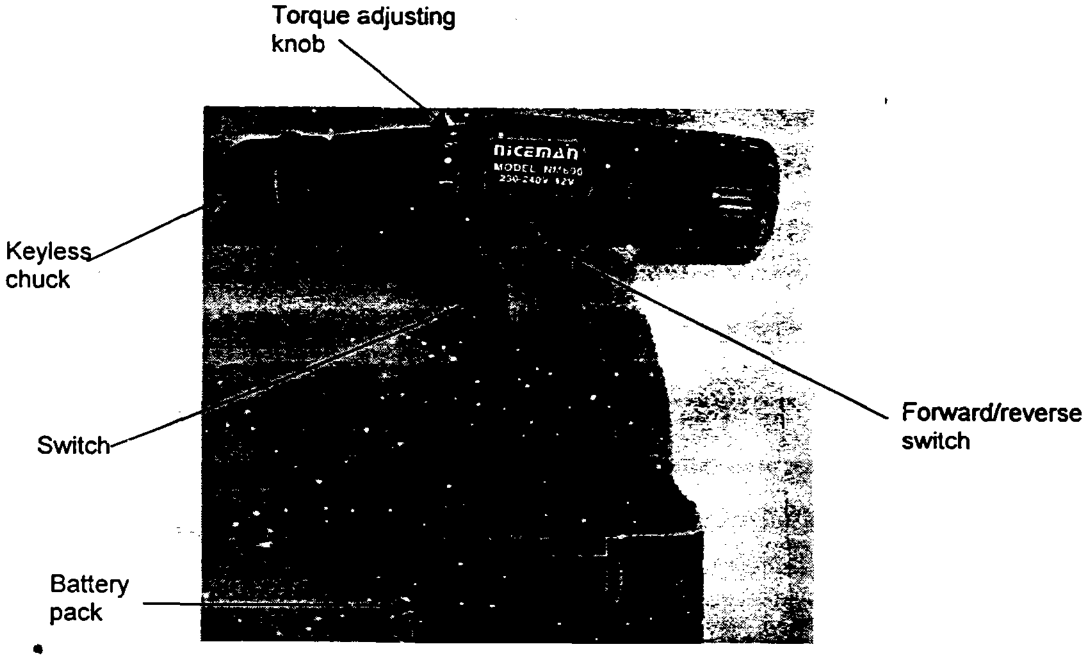

Figure 5.10: Image of cordless drill and driver tool, 'NICEMAN®' model NM600.

The cordless driver tool was used initially to fasten the screw into the composite material without prior drilling process. If the first step does not work, a pilot/lead hole is required in order to fasten the screw to join the fastening members. A pilot hole of certain diameter and depth has to be determined or drilled in order to enable the screw to penetrate into the material. Both undersized and oversized pilot hole will cause problems. The screws are unable to grip the fastening members properly if the pilot hole is oversized while the screws may not be driven in if the hole is undersized. Since various nominal sizes of screws ranging from #3 (2.5146 mm) to #10 (4.826 mm) were used in the fastening study. both their minimum pilot hole diameters and depths were determined. Four drill bit sizes were selected, namely 1.5 mm, 2.0 mm, 2.5 mm and 3.0 mm in diameter. They were used to determine the minimum diameters that allow various nominal size screws to penetrate into the material completely with lowest torque setting. Initially, a wooden stick was used to tie to the drill bits with blue sticky tape so as a distance measured from tip of the drill bits to the stick was arbitrary 2.0 mm as shown in Figure 5.11. The minimum depth of the pilot hole was then determined by trial and error from initial depth of 2.0 mm and increased by 2.0 mm until the material allows the specified nominal size screws to be driven in completely with lowest torque setting. After the pilot hole was drilled, another wooden stick with 3.5 mm in length and 1.5 mm in diameter was put inside the hole and the left out part of the wooden stick was measured in order to confirm that the depth of the pilot hole is same as determined earlier (see Figure 5.12). The minimum hole depths and hole diameters to allow the screw to penetrate completely for various nominal size screws were recorded.

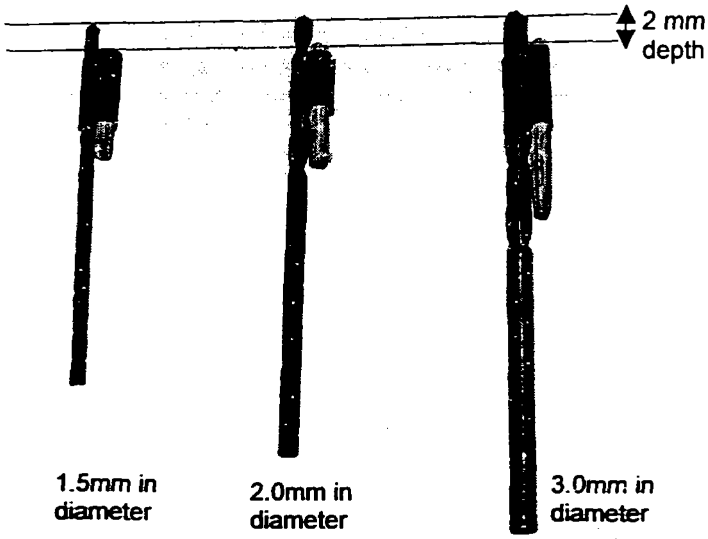

Figure 5.11: Various drill bits with 2.0 mm drill depths indicated by blue sticky tape.

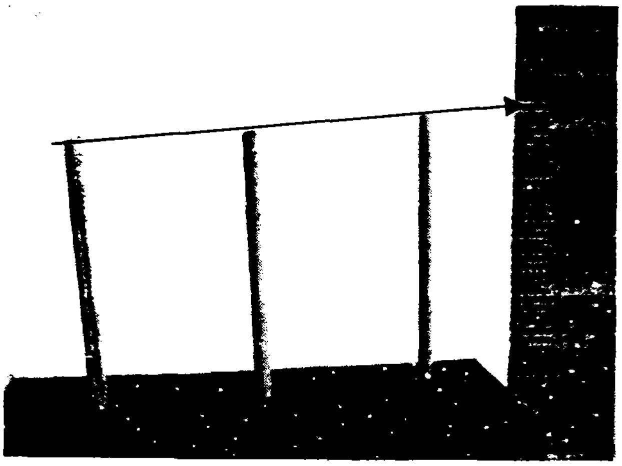

Figure 5.12: The method to determine pilot hole with 2.0 mm depth using wooden stick.

In the fastening study, simple fastening steps were developed which include drilling, countersinking and screw driving processes. A clear centre mark was first made on the material to be drilled using a hole puncher. Then, a proper drill bit and minimum torque setting were selected to create a pilot hole. Finally, countersinking was carried out using proper diameter countersunk tool on the pilot hole. The purpose of using the countersunk bit is to enlarge the top of the hole in order to allow the countersunk head screw to penetrate into the material to obtain a flush surface. These steps were repeated in various fastening studies for the various compositions of the composite materials. Besides, two different types of screws, namely woodscrews and tapping screws were used in the fastening study and the ease of fastening the screws to the composite materials was investigated.

In order to avoid cracking or splitting of the materials, the minimum distance from the center of a fastener to the edge of the member, *a*, the minimum distance from the center of a fastener to the end of the member, *b* as well as the distance between two screws, *S* were determined. These parameters are very important especially during the assembly of full-sized pallet and are illustrated in Figure 5.13.

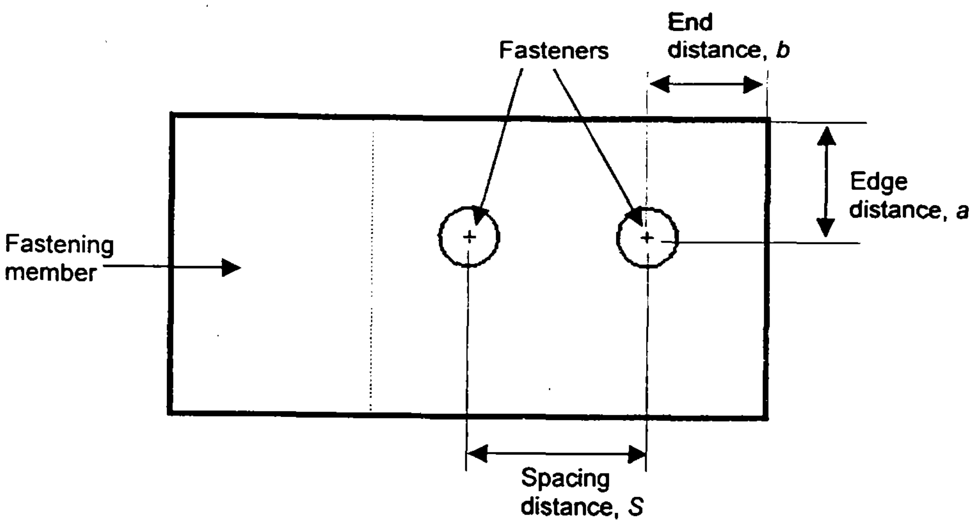

Figure 5.13: Schematic of end distance, edge distance and spacing distance.

The initial edge distance a and end distance b of screws to the fastening member were set to 12.0 mm and were reduced by 1.0 mm gradually until cracking or splitting occurred. Besides, the initial distance between two screws, S, was set to 20.0 mm and was reduced by 2.0 mm gradually until splitting was observed. These investigations will aid in determining the number of fasteners or nominal size of fasteners that can be used for fastening the deck board to the stringer of a full size pallet. The parameters (a, b and S) are important when there is a limitation in dimensions of a deck board. The values of a, b and S of various nominal size screws ranging from #3 to #8 to the fastening member were recorded.

5.4 Results and Discussion

From the initial experiments, it was found that neither woodscrews nor tapping screws can penetrate into the smooth surface of the composite material without pre-drilling a pilot hole. Therefore, pilot holes were drilled using four drill bits of sizes, 1.5 mm, 2.0 mm, 2.5 mm and 3.0 mm as shown in Figure 5.14 in order to determine minimum pilot hole diameter that would allow full penetration of the screw during fastening. The pilot hole depths were determined using 3.5 mm length wooden stick.

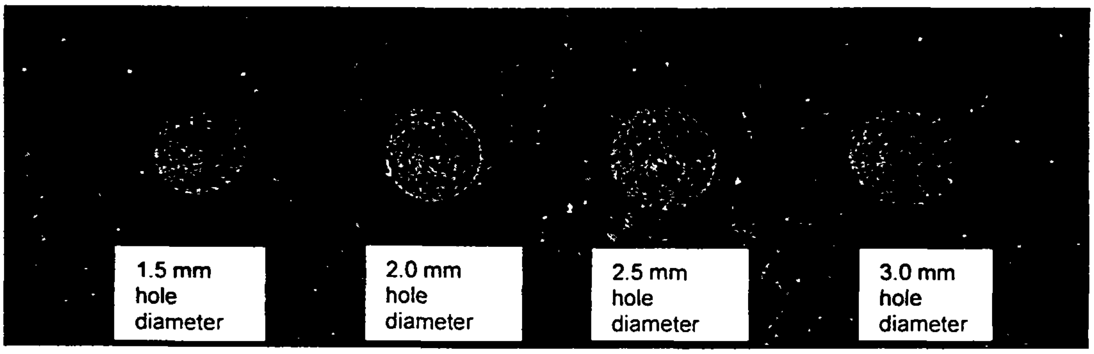

Figure 5.14: Various pilot hole diameters of 1.5 mm, 2.0 mm, 2.5 mm and 3.0 mm used in fastening study.

Table 5.2 shows the results of measurement of the length of screws which penetrate into the member on four different pilot hole diameters when pilot hole depth is set constant to 6.0 mm. 30% wood flour with 70% polypropylene composite materials were used in the study due to its best mechanical properties among the various combinations. For pilot hole diameter of 1.5 mm, the results showed that smaller nominal size of screws can penetrate easily compared to larger nominal size of screws. The ease of penetration of screws can be determined from measurement of the left out part of wooden stick. In other words, more left out part of wooden stick means the screws is more difficult to penetrate into the member with proposed torque setting used in this study. Table 5.2 also shows that penetration of screws of various nominal sizes become easier when pilot hole diameter becomes larger. In this situation, pilot hole diameter of more than 2.5 mm allows the screws to fully penetrate into the member easily. The image of penetration of screws of nominal size #6 and #8 were shown in Figure 5.15(a)-(b).

Table 5.3 shows the results of measurement of the length of screws which penetrate into the member on four different pilot hole depth: 2.0 mm, 4.0 mm, 6.0 mm and 8.0 mm when pilot hole diameter is set constant to 2.5 mm. Again, the results showed that increasing of pilot hole depth allows the screws of various nominal size to penetrate easily especially when pilot hole depth is more than 6.0 mm. In other words, increasing of pilot hole depth improved the ease of penetration of screws to the member.

Table 5.2: The measurement of the length of screws which penetrate into the member on various pilot hole diameter with pilot hole depth = 6.0 mm.

Gauge number, #	Diameter, D, in. (mm)	30%WF:70%PP (by weight fraction) pilot hole depth = 6.0 mm							
		Pilot hole Diameter (mm)							
		1.5	2.0	2.5	3.0	1.5	2.0	2.5	3.0
		Measurement of length of screw which penetrates into the member (mm) Trial 1				Measurement of length of screw which penetrates into the member (mm) Trial 2			
3	0.099 (2.515)	5.7	12.7	12.7	12.7	7.7	12.7	12.7	12.7
4	0.112 (2.845)	4.7	8.7	12.7	12.7	5.7	7.7	12.7	12.7
5	0.125 (3.175)	2.7	7.7	12.7	12.7	2.7	7.7	12.7	12.7
6	0.138 (3.505)	1.7	4.7	12.7	12.7	2.7	3.7	12.7	12.7
8	0.164 (4.166)	0.7	7.7	12.7	12.7	0.7	5.7	12.7	12.7

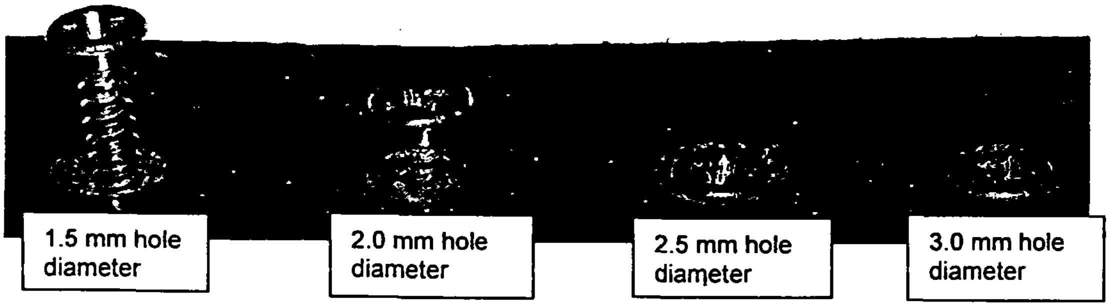

(a)

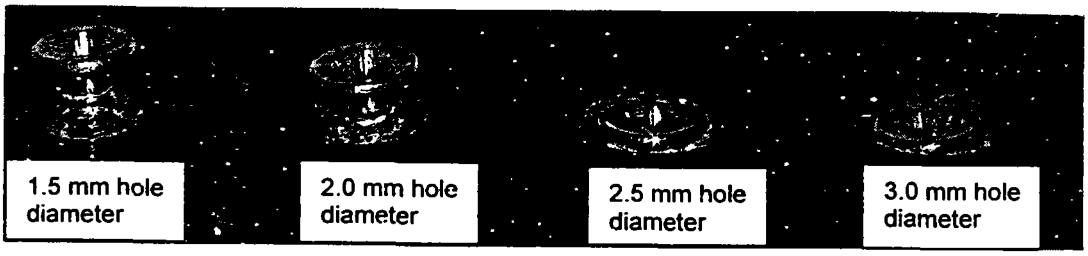

(b)

Figure 5.15: Penetration of screws in various pilot hole diameters (a) screw of nominal size #6, (b) screw of nominal size #8 where pilot hole depth is set to 6.0mm.

Table 5.3: The measurement of the length of screws which penetrate into the member on various pilot hole depth with pilot hole diameter = 2.5 mm.

Gauge number, #	Diameter, D, In. (mm)	30%WF:70%PP (by weight fraction) pilot hole diameter = 2.5 mm							
		Pilot hole depth (mm)							
		2.0	4.0	6.0	8.0	2.0	4.0	6.0	8.0
		Measurement of length of screw which penetrates into the member (mm) Trial 1				Measurement of length of screw which penetrates into the member, (mm) Trial 2			
3	0.099 (2.515)	5.7	6.7	12.7	12.7	6.7	6.7	12.7	12.7
4	0.112 (2.845)	6.7	7.7	12.7	12.7	5.7	6.7	12.7	12.7
5	0.125 (3.175)	6.7	7.7	12.7	12.7	5.7	7.7	12.7	12.7
6	0.138 (3.505)	4.7	12.7	12.7	12.7	5.7	12.7	12.7	12.7
8	0.164 (4.166)	6.7	12.7	12.7	12.7	7.7	12.7	12.7	12.7

During the drilling process, a centre point was marked with a hole puncher and the work piece was clamped properly. Since a lot of the composite chips stick along the drill bit while drilling, the drill bit was withdrawn intermittently to remove or drive out the chips which may block the path during drilling or screw fastening. The drill bit was cleaned before and after the drilling process in order to remove the chips sticking along the flute, which are normally in relatively small pieces. Investigation of the ease of screws using in fastening showed that full thread tapping screws can penetrate into the composite material more easily compared to woodscrews. This is illustrated in Figure 5.16 (a)-(b) which shows that with the minimum torque setting 1 of this cordless driver tool, the tapping screw can be fastened into the material easily, whereas the shank of woodscrew of length 7 mm was left outside the material. Besides, the shank of woodscrew sometimes causes splitting and cracking of the material while it is being driven in. Due to this reason, tapping screws were used for later investigations.

Figure 5.17 (a)-(d) shows the effect of minimum edge distance *a* and end distance *b* of screws with nominal size #4 (2.845 mm) on the fastening members. Table 5.4 shows the results of minimum edge and end distance of screws with various nominal sizes on four different composite materials with increase of filler content in steps of 10% to 40%. It was found out that *a* and *b* more than 8.0 mm would not cause cracking on the composite material with screw of nominal size #8 (4.1656 mm). Besides, minimum *a* and *b* of more than 5.0 mm would not cause cracking on the composite material with screw of nominal size #3 (2.515 mm). In other words, smaller screws can be driven closer to the edge or end of the material than larger ones because they are less likely to cause splitting of material. The results are repeatable except for 40% wood flour with 60% polypropylene composite material. This may due to less homogeneity in this composition. In other words, either larger edge and end distance or smaller nominal size screw required during pallet fabrication using 40%

wood flour -60% polypropylene composite materials in order to avoid cracking of the material.

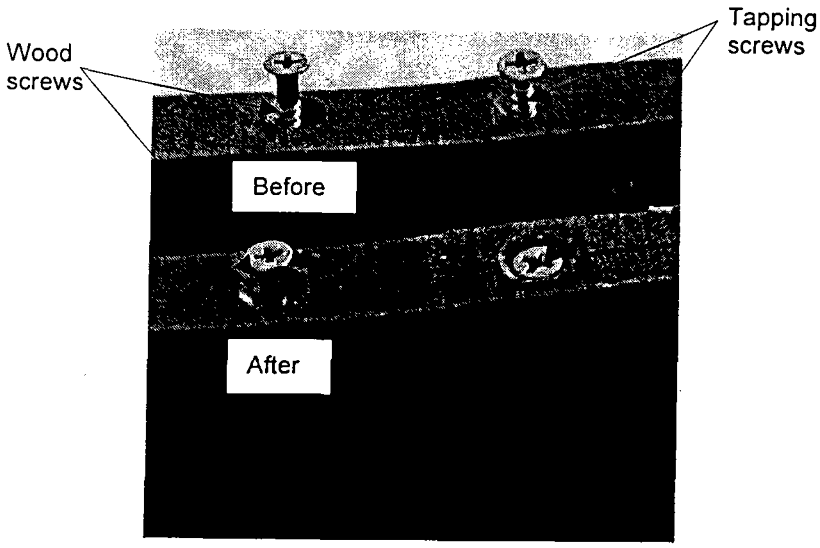

(a)

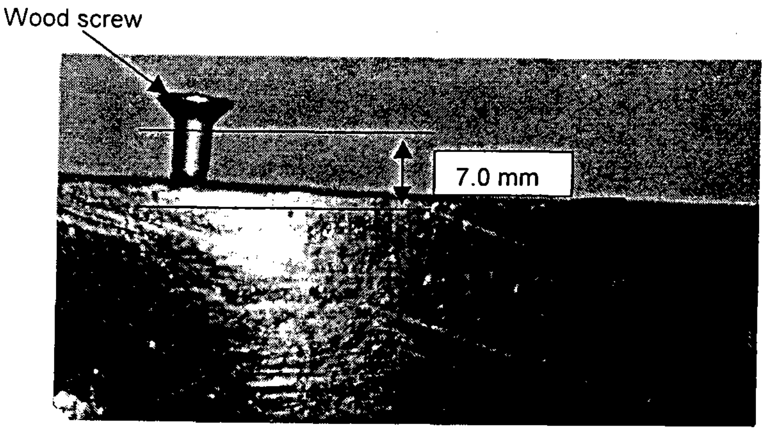

(b)

Figure 5.16: Comparison the ease of fastening between (a) woodscrews and (b) tapping screws.

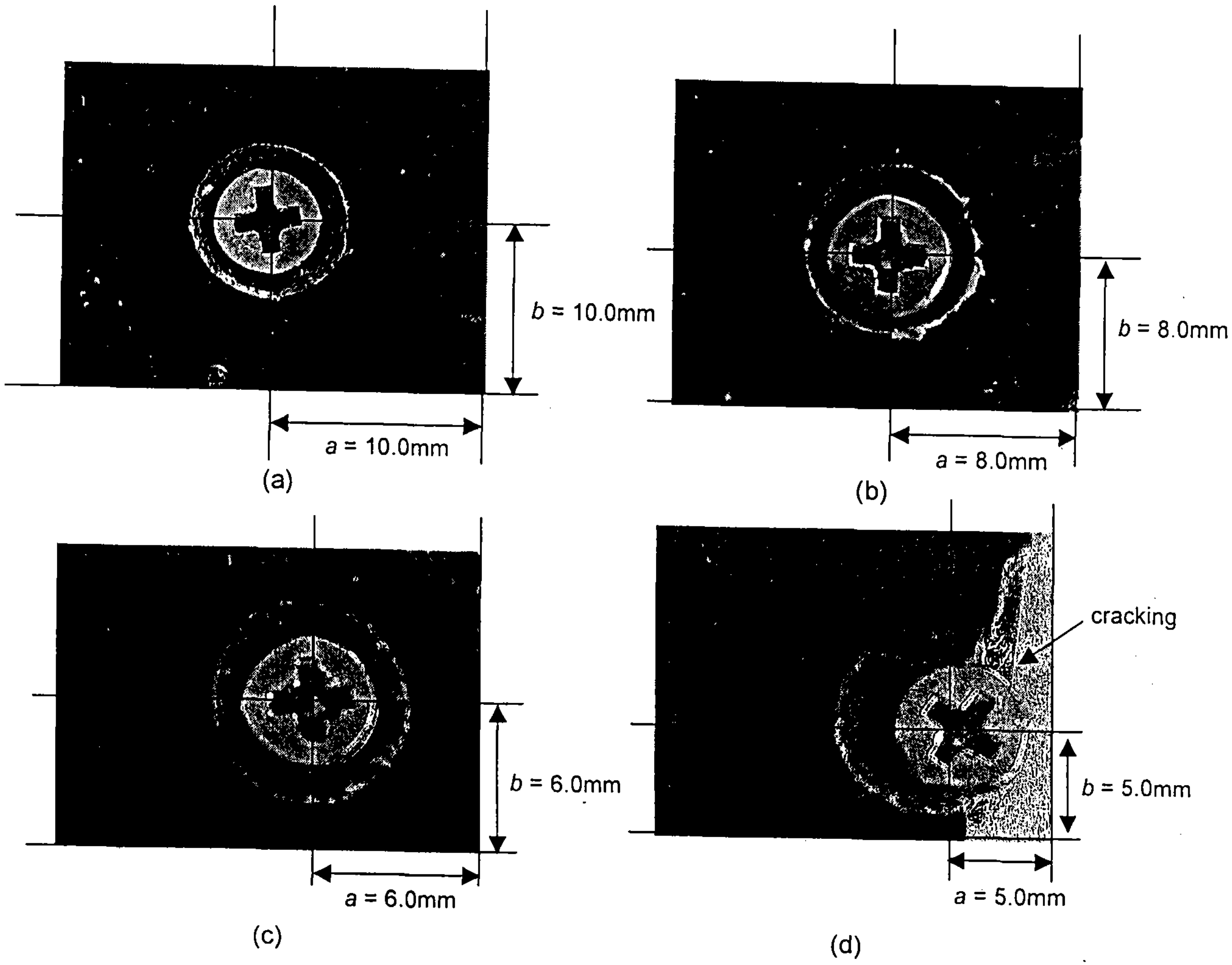

Figure 5.17: Image of the edge distance and end distance of nominal size #4 (2.845 mm) tapping screws.

Table 5.4: The minimum edge and end distance of screw with various screw sizes on four different composite material.

Gauge Number, #	Diameter, D, in. (mm)	10WF:90PP (by weight fraction)				20WF:80PP (by weight fraction)				30WF:70PP (by weight fraction)				40WF:60PP (by weight fraction)			
		Minimum edge distance of screw to the member before cracking, *a* (mm)		Minimum end distance of screw to the member before cracking, *b* (mm)		Minimum edge distance of screw to the member before cracking, *a* (mm)		Minimum end distance of screw to the member before cracking, *b* (mm)		Minimum edge distance of screw to the member before cracking, *a* (mm)		Minimum end distance of screw to the member before cracking, *b* (mm)		Minimum edge distance of screw to the member before cracking, *a* (mm)		Minimum end distance of screw to the member before cracking, *a* (mm)	
		Trial 1, (mm)	Trial 2, (mm)	Trial 1, (mm)	Trial 2, (mm)	Trial 1, (mm)	Trial 2, (mm)	Trial 1, (mm)	Trial 2, (mm)	Trial 1, (mm)	Trial 2, (mm)	Trial 1, (mm)	Trial 2, (mm)	Trial 1, (mm)	Trial 2, (mm)	Trial 1, (mm)	Trial 2, (mm)
3	0.099 (2.515)	5.0	5.0	5.0	5.0	5.0	5.0	5.0	5.0	5.0	5.0	5.0	5.0	6.0	6.0	6.0	6.0
4	0.112 (2.845)	5.0	5.0	5.0	5.0	5.0	5.0	5.0	5.0	5.0	5.0	5.0	5.0	6.0	6.0	6.0	6.0
5	0.125 (3.175)	6.0	6.0	6.0	6.0	6.0	6.0	6.0	6.0	6.0	6.0	6.0	6.0	6.0	7.0	6.0	7.0
6	0.138 (3.505)	8.0	8.0	8.0	8.0	8.0	8.0	8.0	8.0	8.0	8.0	8.0	8.0	8.0	9.0	8.0	9.0
8	0.164 (4.166)	8.0	8.0	8.0	8.0	8.0	8.0	8.0	8.0	8.0	8.0	8.0	8.0	9.0	9.0	9.0	9.0
9	0.177 (4.496)	10.0	10.0	10.0	10.0	12.0	12.0	12.0	12.0	10.0	10.0	10.0	10.0	12.0	12.0	12.0	12.0
10	0.190 (4.826)	10.0	10.0	10.0	10.0	10.0	12.0	12.0	10.0	10.0	10.0	10.0	10.0	12.0	12.0	12.0	12.0

In our fastening study, when the thickness of the fastening member is 15 mm, the edge distance and end distance of the fastener to the member cannot be driven closer than 7.0 mm, i.e. roughly one-half of its thickness of the member. This has similar observation by Soltis (1999) on study of the effect of edge and end distance of nails to the fastening member where nails should not be driven close to the edge or to the end of the fastening member less than one-half the thickness of the member. Besides, it was observed in our fastening study that there is a linear upwards relationship of screw's nominal size to the edge distance and end distance of the screw to the fastening member. Figure 5.18(a)-(b) show the plots of screw gauge number over edge and end distance required during fastening study. By using *linear regression methods*, it shows that screw gauge number has linear relationship to the edge and end distance because the correlation coefficient, R^2 is relatively close to 1.

Figure 5.19 shows the effect of distance between two screws of nominal size #6 (3.505 mm) on 30% wood flour-70% polypropylene composite material. It was observed that the distance between two screws of more than 8.0mm would not cause cracking on the composite material. Table 5.5 shows the minimum spacing distance of screws with various nominal sizes on four different compositions. As mentioned before, this parameter is particularly important especially in determination of the number of screws required in fastening the deck board to the stringer of a pallet. For instance, if the width of deck board or stringer is too small to allow two fasteners of specified nominal size, then only one screw may be used to join the members together due to insufficient distance between two screws on the composite. The observation showed that smaller nominal size of screws has closer space distance.

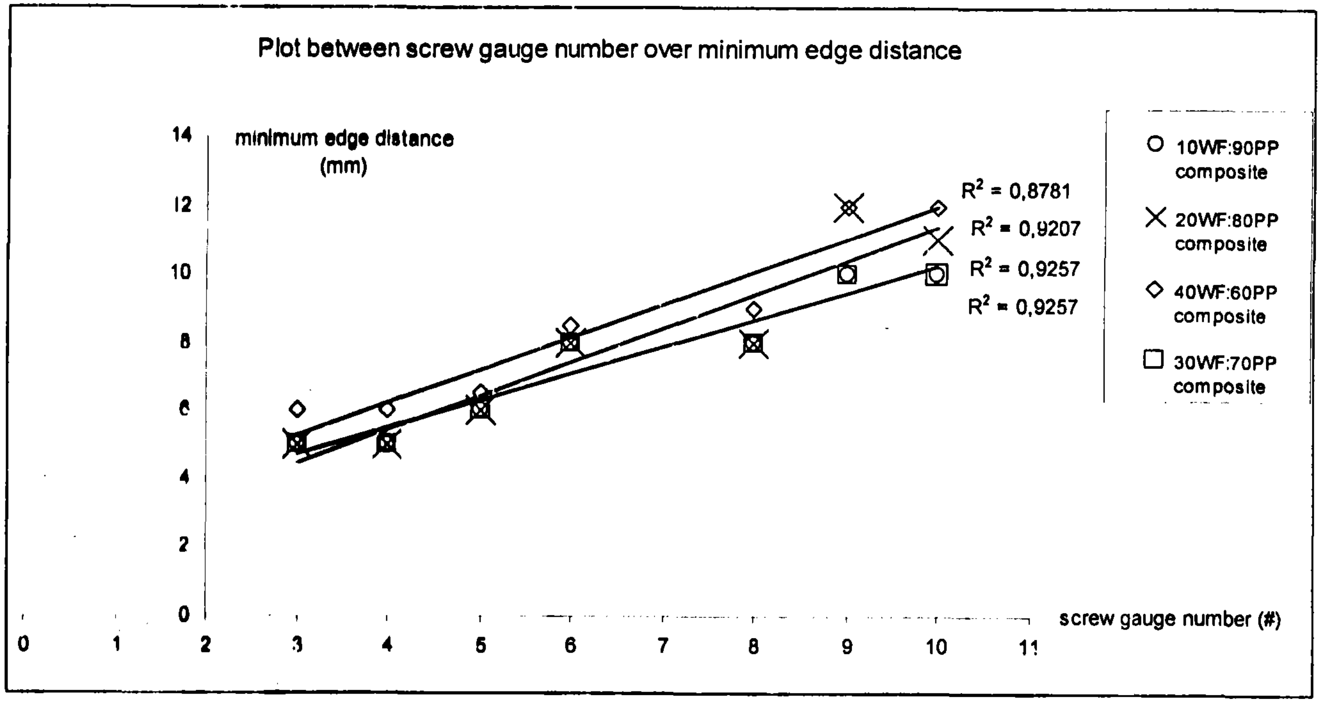

Figure 5.18(a): Plot of various screw gauge number over minimum edge distance of four different composite materials.

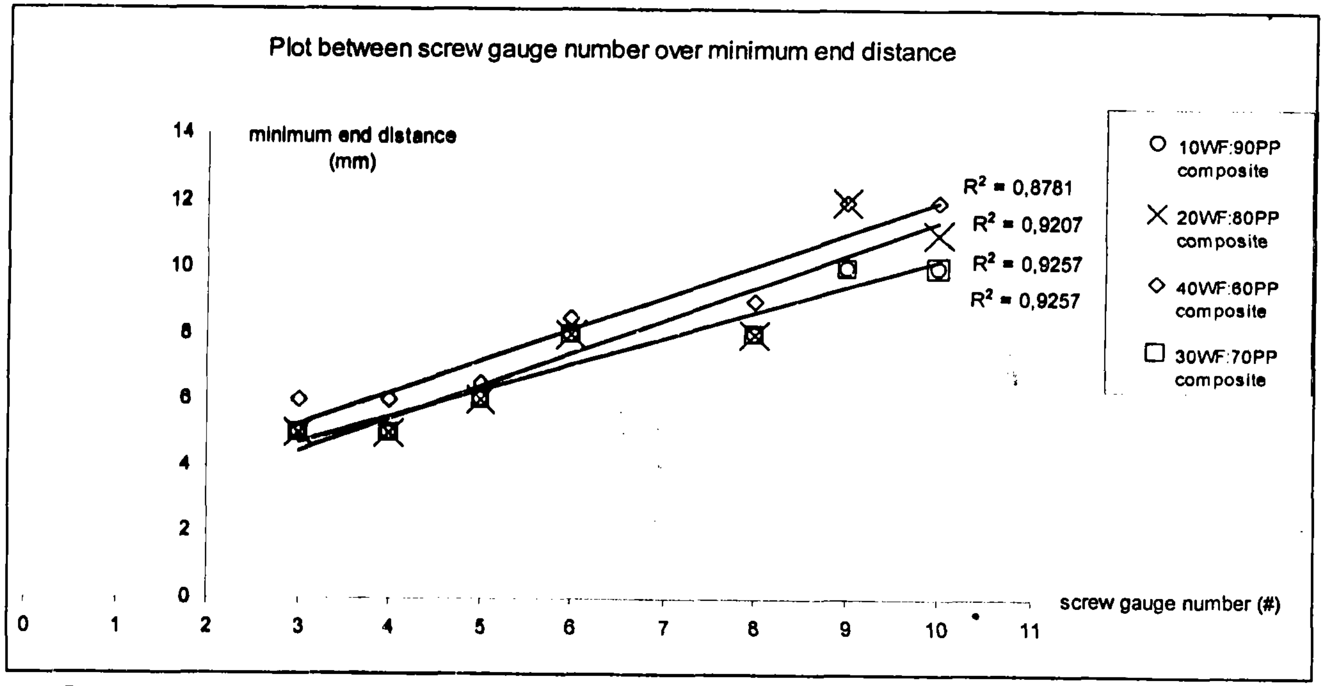

Figure 5.18(b): Plot of various screw gauge number over minimum edge distance of four different composite materials.

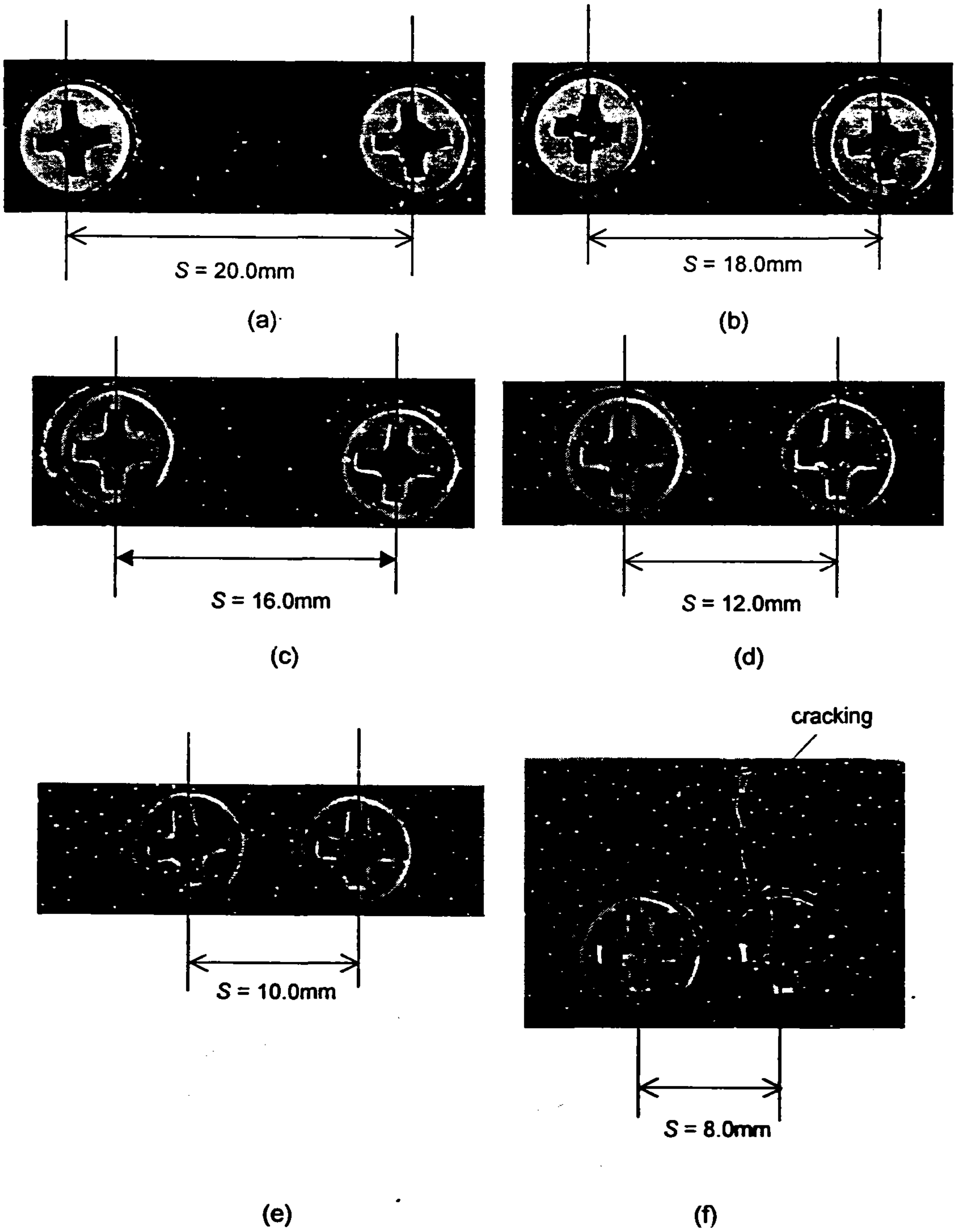

Figure 5.19: The minimum spacing distance between two screws of nominal size #6 (3.505 mm) on 30% wood flour with 70% PP composite materials.

Table 5.5: Spacing distance between two screws of various nominal sizes on four different composite materials.

Gauge Number, #	Diameter, D, in. (mm)	10WF:90PP (by weight fraction) Minimum spacing distance between two screws before cracking, *S* (mm)		20WF:80PP (by weight fraction) Minimum spacing distance between two screws before cracking, *S* (mm)		30WF:70PP (by weight fraction) Minimum spacing distance between two screws before cracking, *S* (mm)		40WF:60PP (by weight fraction) Minimum spacing distance between two screws before cracking, *S* (mm)	
		Trial 1, (mm)	Trial 2, (mm)	Trial 1, (mm)	Trial 2, (mm)	Trial 1, (mm)	Trial 2, (mm)	Trial 1, (mm)	Trial 2, (mm)
3	0.099 (2.515)	5.0	5.0	5.0	5.0	5.0	5.0	6.0	6.0
4	0.112 (2.845)	6.0	5.0	5.0	5.0	5.0	5.0	6.0	6.0
5	0.125 (3.175)	6.0	6.0	6.0	6.0	6.0	6.0	6.0	6.0
6	0.138 (3.505)	7.0	7.0	7.0	8.0	8.0	8.0	7.0	8.0
8	0.164 (4.166)	9.0	9.0	9.0	9.0	9.0	9.0	10.0	10.0
9	0.177 (4.496)	11.0	11.0	11.0	12.0	12.0	12.0	12.0	14.0
10	0.190 (4.826)	12.0	12.0	12.0	12.0	12.0	12.0	14.0	14.0

All the foregoing results, including edge distance, end distance and spacing between two screws are very useful for use in later assembly of the full size pallet. The screws with various nominal sizes ranging from #3 (2.5146 mm) to #10 (4.826 mm) could be used in an assembly of full size pallet. The main problem is limitation in length of screws, whereby maximum length of screws with nominal size less than #8 is only 1.5 inch (38.1 mm). These lengths of screws (#3-#6) are not suitable to be used in an assembly of full size pallet because minimum height of pallet is 3.25 inch (83.0 mm) due to standard thickness of fork tine (83.0 mm) of pallet jack. In the study, tapping screws with nominal sizes of #8 (4.1656 mm) to #10 (4.826 mm) were used in an assembly of a prototype or scaled down pallet model as shown in Figure 5.20. From the study, it shows that fastening of tapping screw (nominal size #9) with length of 2.25 inch (57.15 mm) to the deck board of 15mm in length and stringer of 50 mm in length with lower torque setting without difficulty. Figure 5.21(a)-(b) show the fastening of scaled down deck board and stringer using screw size #6 and #8. The study showed that screw with nominal sizes ranges from #3 (2.5146 mm) to #6 (3.505 mm) and length of 0.5 inch (12.7 mm) is suitable to be used in an assembly of one-fifth scaled down pallet model that would be used to verify the prediction of the finite element model using non-contact optical measurement. This is because screws of nominal size #8 would cause cracking to the member when fastening to the scaled down deck board with stringer as shown in Figure 5.21(b). Nevertheless, simple fastening steps (pre-drilling, countersinking and screw driving) are repeatable on four different compositions of natural fiber-reinforced composite materials with increase of wood filler contents from 10% to 40% (by weight fraction). The only difference is while increasing the wood filler contents, the composite materials become more brittle and many chips were formed when drilling a hole on these composites. This is especially obvious on 40% wood fillers-60% polypropylene composite materials. These chips should be avoided especially during drilling deep hole since they tend to pack in the flutes and prevent heat from being conducted away.

Figure 5.20: Fastening of deck board and stringer in the fastening study.

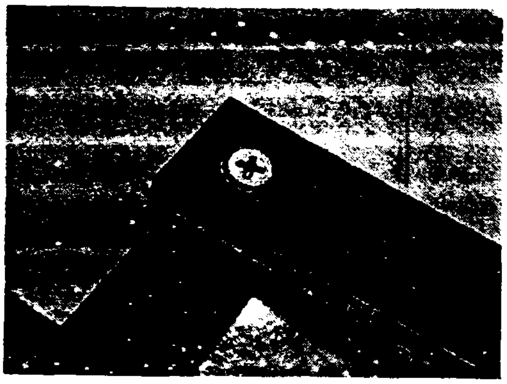

(a)

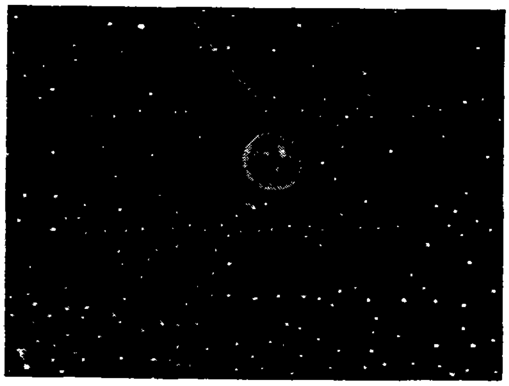

(b)

Figure 5.21: Fastening of (a) #6 and (b) #8 nominal size tapping screws on scaled down deck board and stringer.

5.5 Summary

As a conclusion, the fastening study shows that it is not possible to use woodscrew / tapping screw to fasten into the composite materials without pre-drilling process. A pilot hole / guide hole with diameter of 2.5 mm and depth of more than 6.0 mm is suitable for screws with nominal sizes ranges from #3 (2.515 mm) to #8 (4.166 mm) to penetrate into the composite materials without difficulty with minimum torque setting of NICEMAN® model NM600 driver tool. Besides, minimum torque setting of this driver tool was used in order to prevent driving the screw too deep or causing damage to the tool. Moreover, excessive torque of the driver tool will not only cause damage to the head screw but also cause to thread stripping.

Investigation of the ease of penetration of screws to the fastening member showed that tapping screws with full self drilling threads are more suitable to be used in fastening compared to wood screws. This is because the shank of woodscrew was left outside the composite when using the proposed minimum torque of driver tool compared to tapping screw.

A simple fastening procedure with a cycle of pre-drilling, countersinking and screw driving was used and the screws could be fastened to the composite materials easily and were repeatable. Investigation of the minimum value of *a* and *b* of various nominal sizes screw (#3 to #10) showed that smaller nominal size screws can be driven closer to the edge compared to larger one. Generally, the edge and end distances of screw to the member are roughly one-half of the thickness of fastening member. Besides, the minimum spacing between two screws is increased if the nominal size of screw increased. For instance, minimum spacing between two screws of nominal size #3 was determined as 5.0 mm without causing cracking whereas minimum spacing between two screws of nominal size #8 was observed as 9.0mm without causing cracking.

Again, tapping screws of nominal size ranges from #8 to #10 with length of 2 inch (50.8 mm) to 2.25 inch (57.15 mm) are suitable to be used in an assembly of full size pallet due to minimum required height of pallet must be more than 3.25 inch (roughly 83.0 mm). Besides, tapping screws with nominal sizes range from #3 to #6 and length of 0.5 inch (12.7 mm) are suitable to be used in an assembly of one-fifth scaled down pallet model for optical measurement.

CHAPTER 7

STUDY OF PALLET DEFORMATION USING EXPERIMENTAL AND FEA ANALYSIS

7.0 Introduction

Comparative study of static deformation of one-fifth scaled wood based composite pallet was done between experimental and FEA analysis in order to ensure the validity of FEA for product design of this composite material. One-fifth scaled dimension of composite pallet was previously determined as 240 mm (L) × 200 mm (W) × 20 mm (H) from full size pallet in Chapter 4 (refer Table 4.4). The dimensions of the pallet model needs to be modified after fastening study. Besides, this chapter also presents the correct way for fringe numbering in order to achieve closer agreement between experimental and FEA results. The purpose of this experiment is try to replace the testing of mechanical behaviour of the pallet with computer modeling and reduces involvement of fabrication of too many prototype of pallet in field testing.

7.1 Modification of One-Fifth Scaled Pallet Model

The width of the stringer of one-fifth scaled pallet model needs to be modified after fastening study in order to match the appropriate nominal size of screws selected for scaled down pallet model, which is from #3 (2.515 mm) to #6 (3.505 mm). The results from fastening study showed that minimum end and edge distance to the fastening member for nominal size screws from #3 to #6 is 5.0 mm to 8.0 mm and with this reason, the width of the stringer is modified from 6.0 mm to 13.0 mm in order to avoid cracking of the material while assembly of the pallet model. Figure 7.1(a) and (b) show the images of one-fifth scaled pallet model; with and without sprayed in color. Table 7.1 shows the detailed dimension of this scaled down pallet model including where the width of stringer is modified.

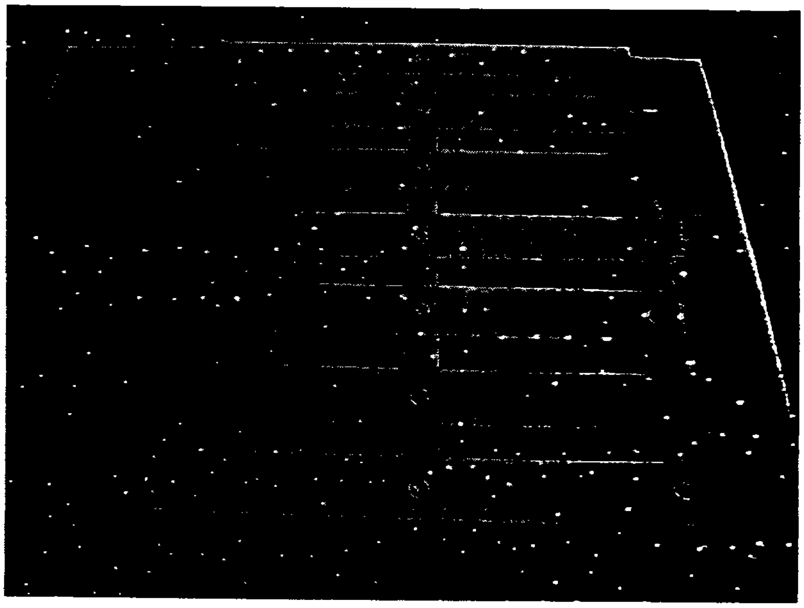

(a)

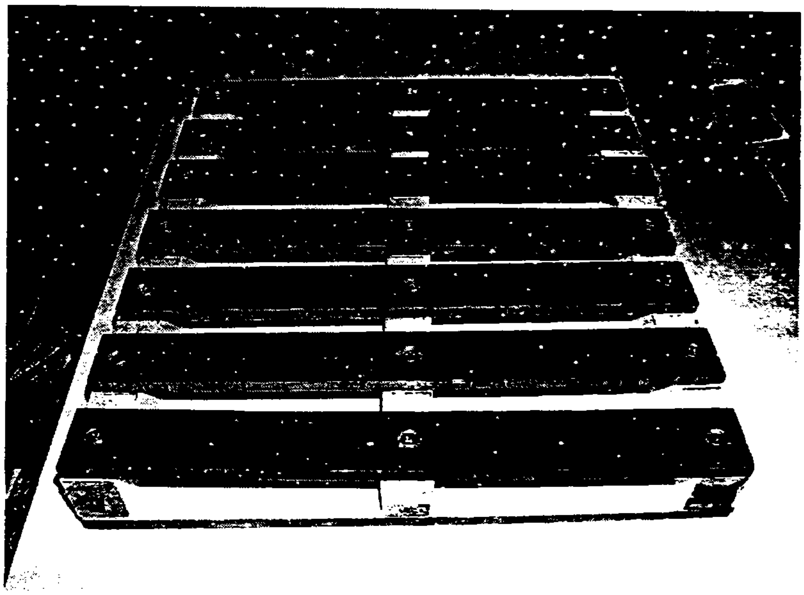

(b)

Figure 7.1: Image of wood based composite pallet model (a) with sprayed colour, (b) without sprayed colour.

Table 7.1: Detailed dimension of full size and one-fifth scaled down pallet.

Name of part	Quantity	Dimensions (mm)	Scaled down Dimensions (mm)
Top deck board	7	1000 (L) × 115 (W) × 16 (H)	200 (L) × 23 (W) × 4 (H)
Bottom deck board	7	1000 (L) × 115 (W) × 16 (H)	200 (L) × 23 (W) × 4 (H)
Stringer	3	1200 (L) × 6 (W) × 100 (H)	240 (L) × 13 (W) × 20 (H)

7.2 Experimental Set-up

Figure 7.2 shows the image of composite pallet model under a total static load of 20.5 kg. The pallet was placed to lean against the rig at a small tilted angle of 2.43° during optical measurement. Fringes are easily formed with this tilted angle; else larger load is required to create these fringes. Application of larger load is not encouraged due to possible damage to the pallet model. Two images were captured, one without applying the load while the other after applying the load by stacking three load bars of 6.6 kg each (see Figure 7.3). Figure 7.4 shows the schematic diagrams of the experimental setup of scaled down pallet model, which is identical to experimental set-up for aluminum plate, except the pallet was placed at small tilted angle. The distances between projector and the pallet and camera to the pallet were 1090 mm and 1280 mm respectively. The heights between projector and the pallet and camera to the pallet were 420 mm and 280 mm respectively.

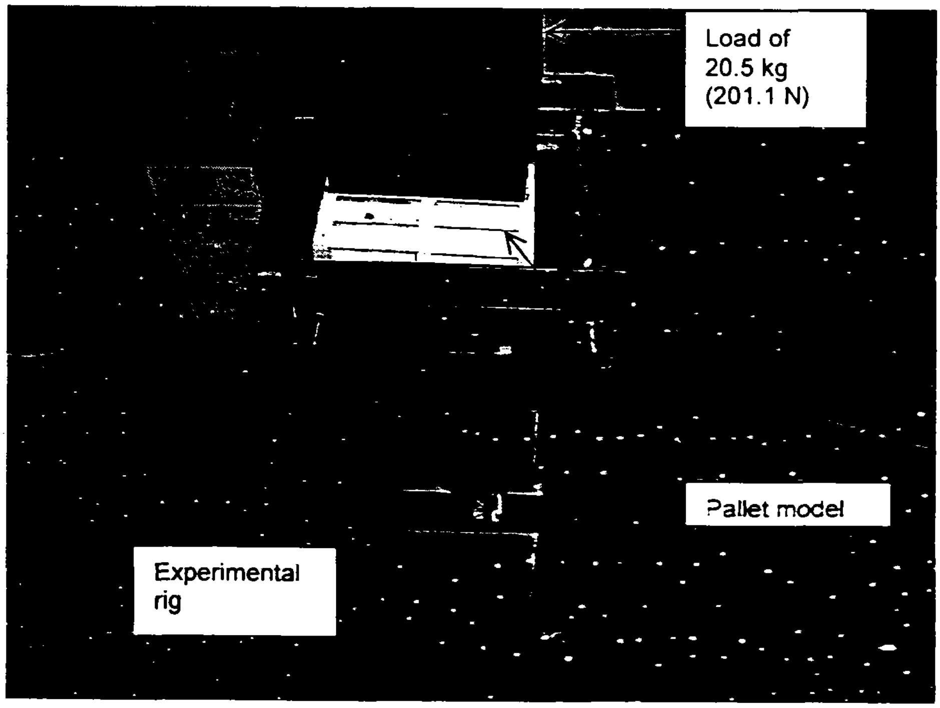

Figure 7.2: Image of pallet model under static load.

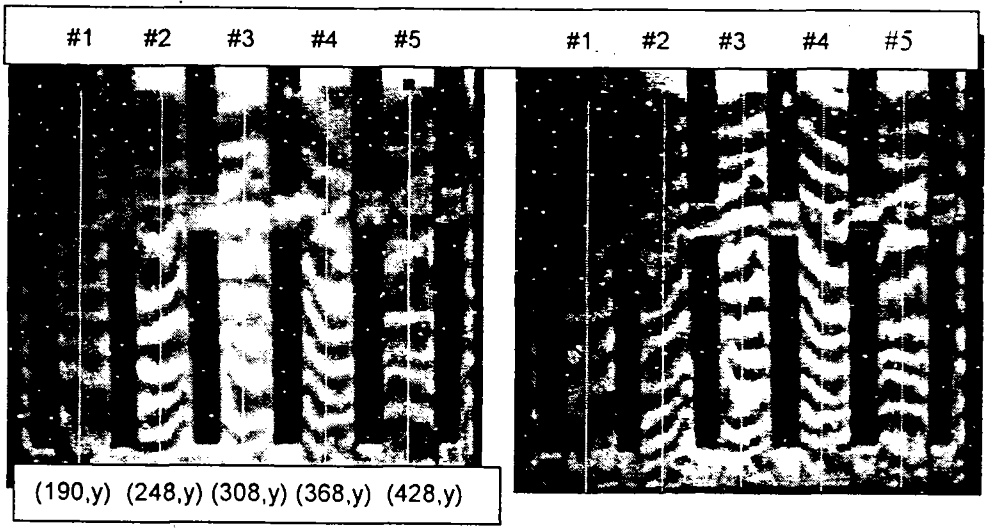

(a) (b)

Figure 7.3 Fringes patterns formed from (a) tilted plate without loading, (b) tilted plate with loading.

A solid model of composite pallet with dimensions 240 mm (L) × 200 mm (W) × 20 mm (H) was created using *SolidWorks* modeler and FEA analysis was carried out to find the deflection of the pallet under a load of 201.1 N. The load was converted to effective pressure applied on the three top deck boards as 14700 Pa as shown in Figure 7.5. Simulation of the pallet was same as the condition in experiment where front part of the pallet was assumed as point constraint under ball bearing while back part of the plate was set as area constraint. Input mechanical properties referred to 30% WSD (100 μm)-70% PP composite: MOE = 2.7564×10^9, UTS = 1.495×10^7 and density = 1013 kg/m^3.

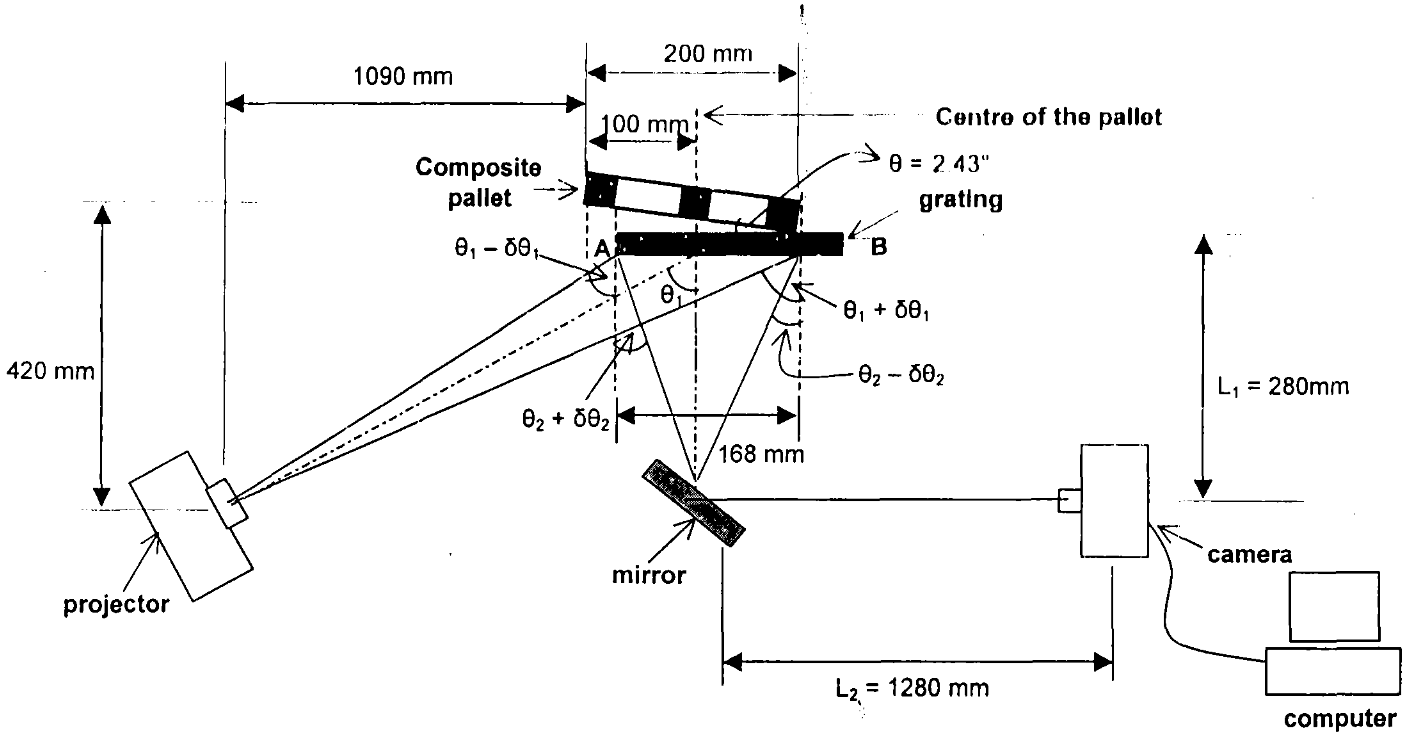

Figure 7.4: A schematic diagram of experimental set-up for tilted pallet model.

For experimental data, line profile was drawn on every strip of bottom deck board and analyzed using *Matrox Inspector* software. Total of 4 sections (Line profiles were analyzed starts from (190,65) to (190,355) and end at (368,65) to (368,355)). Centre point of coordinate-x and y of each fringes were recorded and deflection of the pallet, d, was calculated based on the theory of

$$d = \frac{np}{\tan\theta_i + \tan\theta_v} \tag{7.1}$$

where n is the fringe number starts from 1,2,3,...n; *p* is the pitch of the grating which is equal to 1 mm in this experiment; θ_i is the illumination angle while θ_v is the viewing angle.

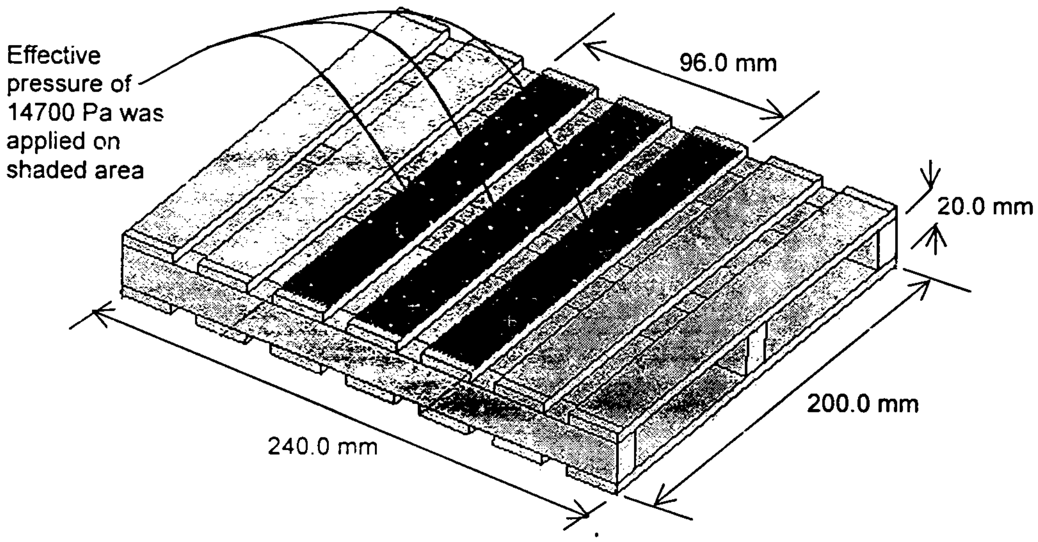

Figure 7.5: Pallet model under static load from FEA analysis.

The centre of the projection angle was assumed to be the centre of the pallet (see Figure 7.6 (a)) during calculation even though the pallet model was placed at a small tilted angle of 2.43°. Since the inclined angle is small, sometimes calculation could be solved based on deflection's calculation of the pallet without tilting (see Figure 7.6 (b)). Pixel coordinates were then transformed to actual world coordinates using scaling factor determined earlier, that is 1.7262 pixels/mm and 1.6630 pixels/mm for axis-y and axis-x respectively. Subtraction was done on the distance measured from pallet to the grating obtained from image of initial pallet without loading and pallet after loading. Subtraction data was used as input to the *Stanford Graphics* software to generate a common grid using *polynomial fitting* order 4, one of the common used interpolation methods before comparing with FEA result. The reference point for this case was determined as (108,15).

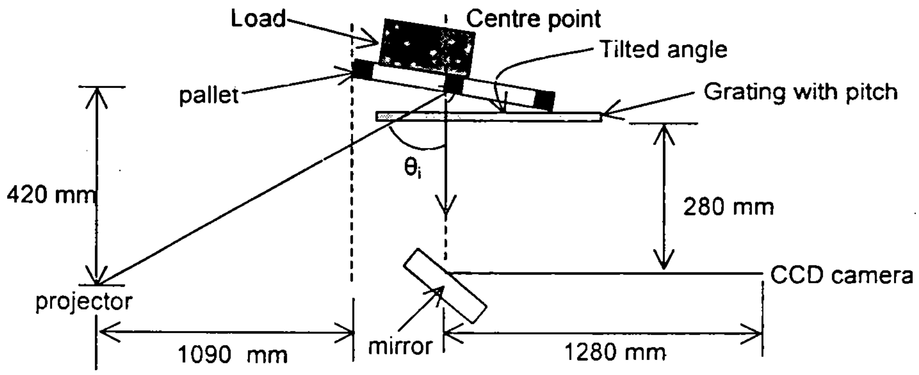

Figure 7.6 (a): A diagram of tilted pallet analysis where center of projection was assumed at center of the pallet.

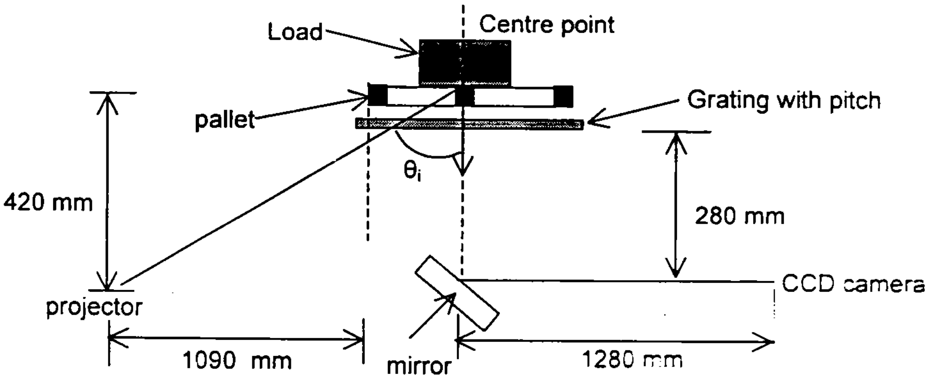

Figure 7.6 (b): Calculation of pallet in normal situation.

Besides calculation of the distance measured from the plate to the grating, identifying of correct fringe numbering, n is very important in order to obtain correct distance measured from the plate to the grating. Figure 7.7 (a) and (b) show the diagram of the plate viewing from the back view and imaginary plane of the fringes were formed when the plate's shadow superimposed with the grating. These diagrams could aid in explaining the way of identifying fringe numbers that were formed on the images.

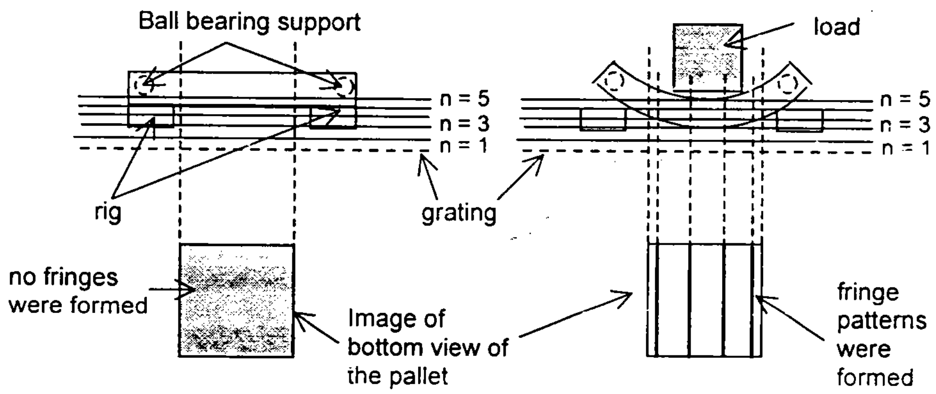

Figure 7.7: The diagram from back view of the aluminum plate (a) without loading, (b) with loading.

7.2.1 Results and Discussion

Figure 7.8 shows the way of identifying the fringe number from the image. From image of pallet after loading, the fringe which connects to the end at both side of the restraint points represent points having deflection, z = 0. Fringe number at this position is identified and used as reference in image of pallet before loading. For image of pallet before loading, the initial fringe number starts at fringe number identified from image of pallet after loading + 1.

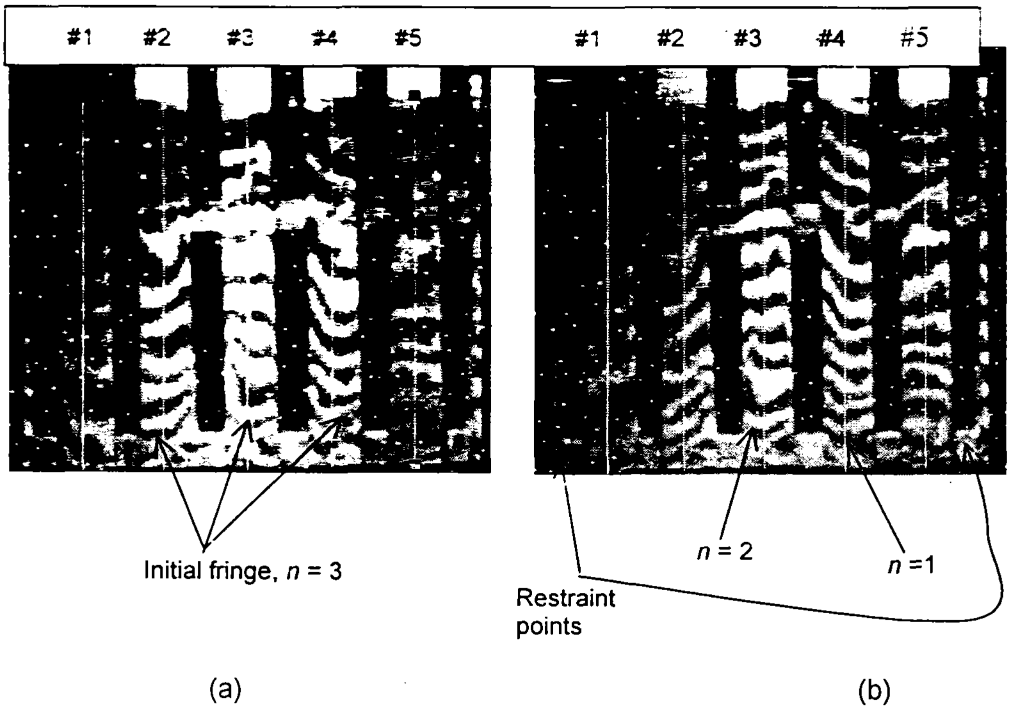

Figure 7.8: Identification of the fringe number from (a) Image before loading, (b) Image after loading.

The raw data of five deck boards of the pallet with and without loading are shown in Appendix G. *Polynommial fitting* of order 4 was used in order to have a common grid between data from pallet with and without loading. Figure 7.9 (a) to (d) show the 2-dimensional plot of coordinate-y over distance measured from stringer of the pallet with and without loading. Subtraction was done after *polynomial fitting*, and the value from subtraction, or deflection profile of experimental and FEA results was compared at Table 7.2 (a) to (d). The differences of deflection profile between experimental and modeling data were also recorded at Table 7.2 (a) to (d). Figure 7.10 (a) to (d) show the 2-dimensional plot of coordinate-y over deflection profile between experimental and modeling data. The deflection profile of pallet model from FEA analysis is shown in Figure 7.11.

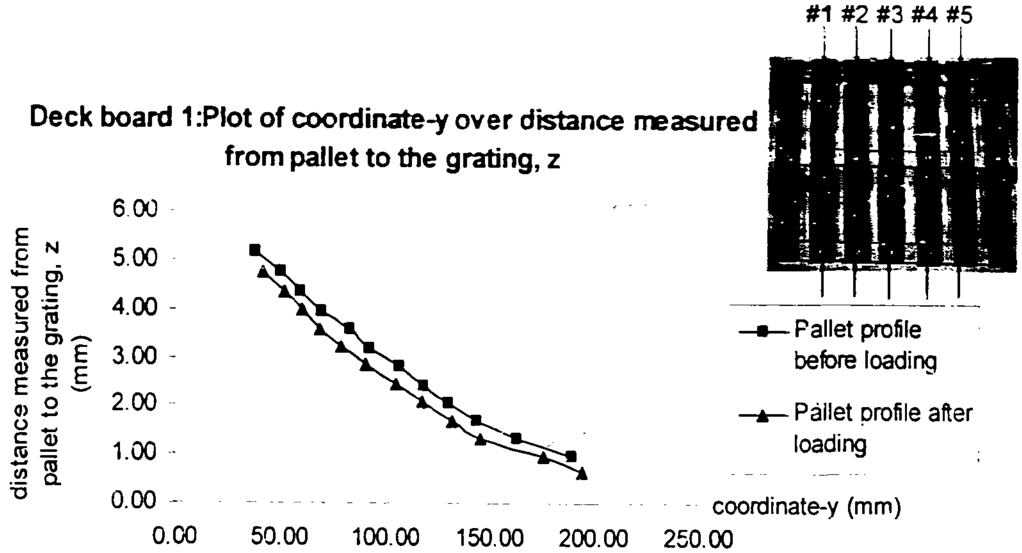

Figure 7.9(a): Plot of coordinate-y over distance measured from first deck board of pallet to the grating with and without loading before *polynomial fitting*.

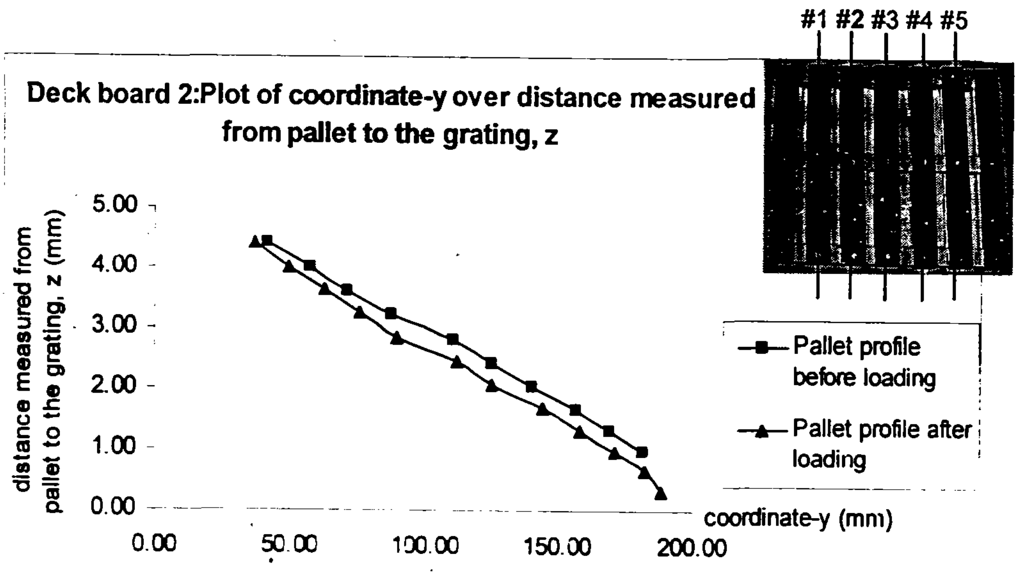

Figure 7.9(b): Plot of coordinate-y over distance measured from second deck board of pallet to the grating with and without loading before *polynomial fitting*.

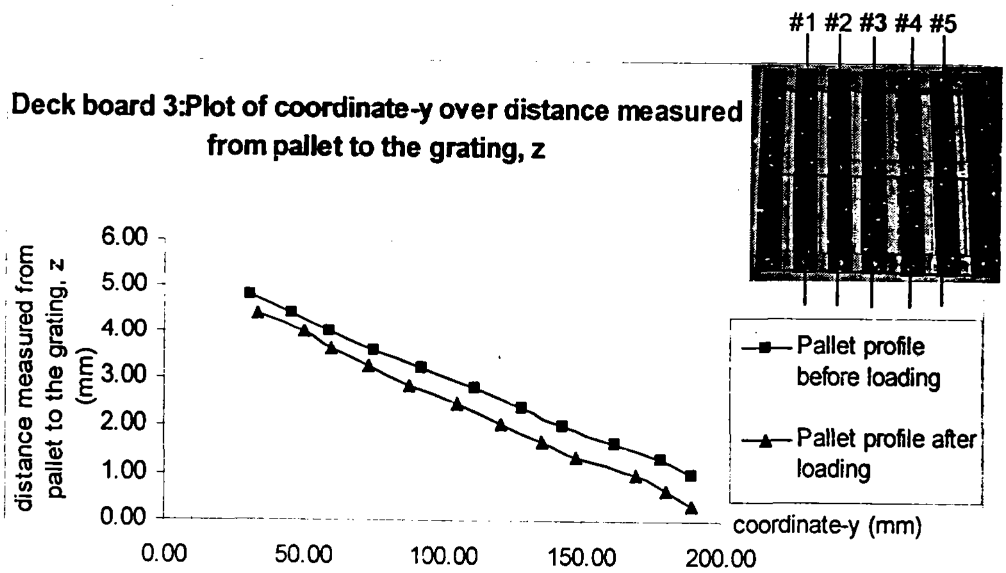

Figure 7.9(c): Plot of coordinate-y over distance measured from third deck board of pallet to the grating with and without loading before *polynomial fitting*.

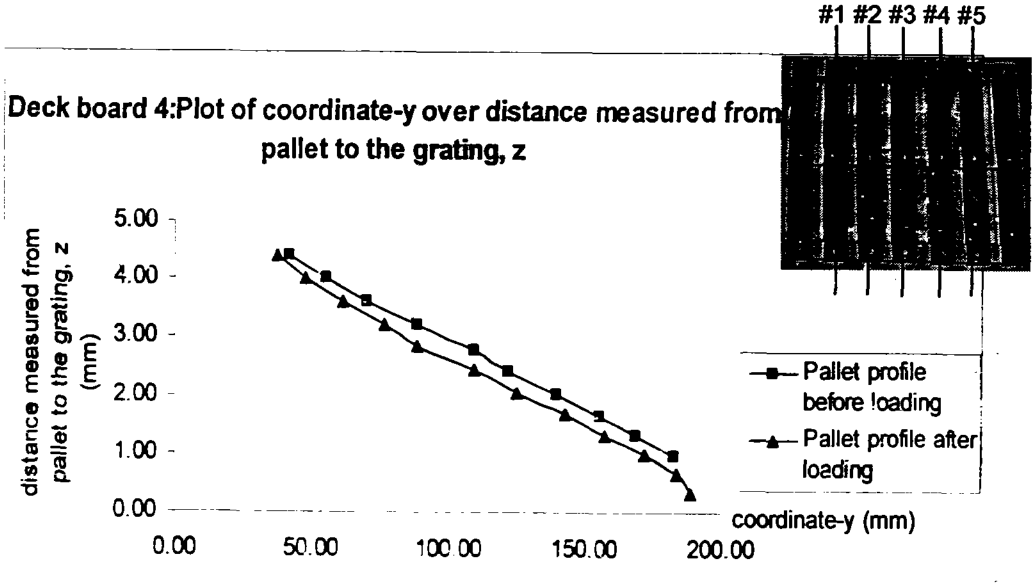

Figure 7.9(d): Plot of coordinate-y over distance measured from fourth deck board of pallet to the grating with and without loading before *polynomial fitting*.

Table 7.2(a): Experimental and modeling data of the first deck board of the pallet under static load and their differences in deflection.

	Experimental data of the pallet after loading		FEA data of the pallet after loading		Differences
	x (mm)	z_0 (mm)	x (mm)	z_1 (mm)	$\lvert z_2$ (mm)$\rvert$
#Line1 Deck board 1 from (190,65) to (190,355)	10.00	-0.08	10.00	-0.13	0.05
	20.00	-0.11	20.00	-0.14	0.03
	30.00	-0.17	30.00	-0.17	0.00
	40.00	-0.23	40.00	-0.21	0.02
	50.00	-0.29	50.00	-0.26	0.04
	60.00	-0.35	60.00	-0.30	0.06
	70.00	-0.40	70.00	-0.33	0.07
	80.00	-0.43	80.00	-0.36	0.08
	90.00	-0.45	90.00	-0.37	0.08
	100.00	-0.44	100.00	-0.37	0.08
	110.00	-0.42	110.00	-0.35	0.07
	120.00	-0.38	120.00	-0.32	0.06
	130.00	-0.33	130.00	-0.28	0.05
	140.00	-0.27	140.00	-0.23	0.04
	150.00	-0.22	150.00	-0.18	0.04
	160.00	-0.18	160.00	-0.14	0.04
	170.00	-0.16	170.00	-0.10	0.06

Table 7.2(b): Experimental and modeling data of the second deck board of the pallet under static load and their differences in deflection.

	Experimental data of pallet after loading		FEA data of pallet after loading		Differences
	x (mm)	z_0 (mm)	x (mm)	z_1 (mm)	$\lvert z_2$ (mm)$\rvert$
#Line2 Deck board 2 from (248,65) to (248,355)	10.00	-0.28	10.00	-0.21	0.07
	20.00	-0.19	20.00	-0.22	0.04
	30.00	-0.15	30.00	-0.25	0.11
	40.00	-0.14	40.00	-0.29	0.15
	50.00	-0.17	50.00	-0.33	0.17
	60.00	-0.20	60.00	-0.37	0.17
	70.00	-0.24	70.00	-0.41	0.16
	80.00	-0.28	80.00	-0.43	0.15
	90.00	-0.31	90.00	-0.44	0.13
	100.00	-0.33	100.00	-0.44	0.11
	110.00	-0.33	110.00	-0.42	0.09
	120.00	-0.32	120.00	-0.39	0.06
	130.00	-0.31	130.00	-0.35	0.04
	140.00	-0.29	140.00	-0.30	0.02
	150.00	-0.27	150.00	-0.25	0.02
	160.00	-0.26	160.00	-0.20	0.06
	170.00	-0.27	170.00	-0.17	0.11

Table 7.2(c): Experimental and modeling data of the third deck board of the pallet under static load and their differences in deflection.

	Experimental data of pallet after loading		FEA data of pallet after loading		Differences
	x (mm)	z_0 (mm)	x (mm)	z_1 (mm)	$\lvert z_2$ (mm)$\rvert$
#Line3 Deck board 3 from (308,65) to (308,355)	10.00	-0.4091	10.00	-0.2475	0.16
	20.00	-0.3277	20.00	-0.2572	0.07
	30.00	-0.2890	30.00	-0.2849	0.01
	40.00	-0.2824	40.00	-0.3226	0.04
	50.00	-0.2983	50.00	-0.3638	0.06
	60.00	-0.3286	60.00	-0.4028	0.07
	70.00	-0.3663	70.00	-0.4350	0.07
	80.00	-0.4059	80.00	-0.4572	0.05
	90.00	-0.4430	90.00	-0.4670	0.03
	100.00	-0.4746	100.00	-0.4632	0.01
	110.00	-0.4989	110.00	-0.4459	0.05
	120.00	-0.5154	120.00	-0.4160	0.10
	130.00	-0.5249	130.00	-0.3757	0.14
	140.00	-0.5295	140.00	-0.3282	0.20
	150.00	-0.5327	150.00	-0.2780	0.25
	160.00	-0 5390	160.00	-0.2304	0.31
	170.00	-0.5545	170.00	-0.1921	0.36

Table 7.2(d): Experimental and modeling data of the fourth deck board of the pallet under static load and their differences in deflection.

	Experimental data of pallet after loading		FEA data of pallet after loading		Differences
	x (mm)	z_0 (mm)	x (mm)	z_1 (mm)	$\|z_2$ (mm)$\|$
#Line4 Deck board 4 from (368.65) to (368,355)	10.00	-0.3841	10.00	-0.2139	0.17
	20.00	-0.2372	20.00	-0.2245	0.02
	30.00	-0.1652	30.00	-0.2531	0.08
	40.00	-0.1473	40.00	-0.2918	0.14
	50.00	-0.1651	50.00	-0.3339	0.16
	60.00	-0.2030	60.00	-0.3736	0.17
	70.00	-0.2482	70.00	-0.4066	0.15
	80.00	-0.2908	80.00	-0.4293	0.14
	90.00	-0.3233	90.00	-0.4396	0.12
	100.00	-0.3413	100.00	-0.4361	0.10
	110.00	-0.3429	110.00	-0.4189	0.08
	120.00	-0.3291	120.00	-0.3891	0.06
	130.00	-0.3035	130.00	-0.3487	0.05
	140.00	-0.2726	140.00	-0.3012	0.03
	150.00	-0.2456	150.00	-0.2509	0.00
	160.00	-0.2344	160.00	-0.2034	0.03
	170.00	-0.2536	170.00	-0.1653	0.08

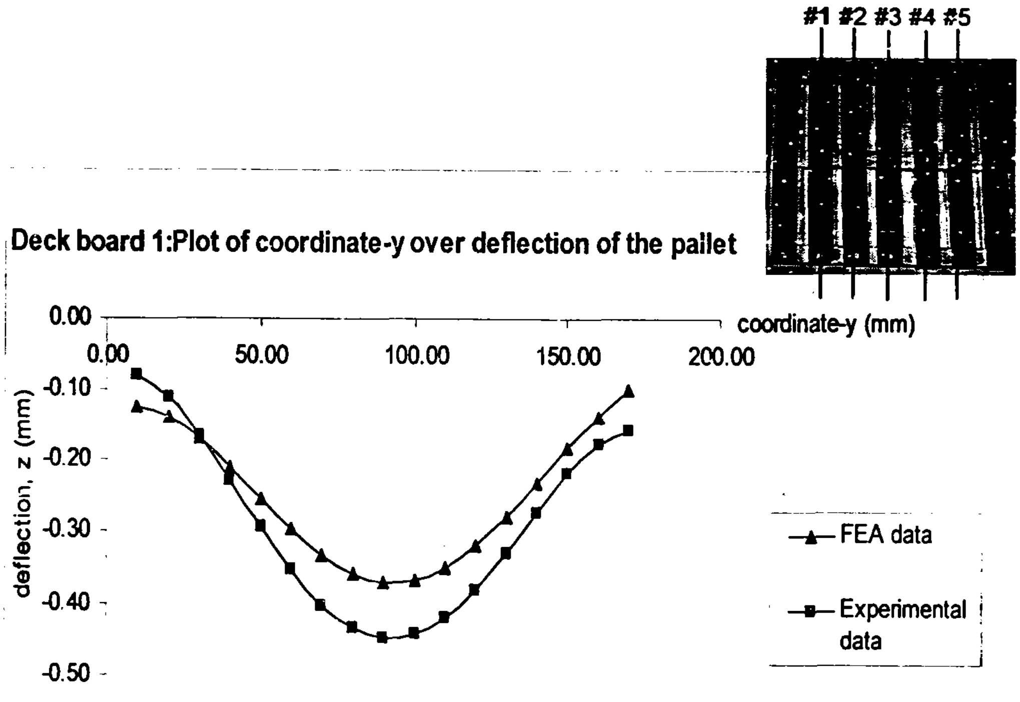

Figure 7.10(a): Comparative study of the deflection of the pallet between experimental and modeling data.

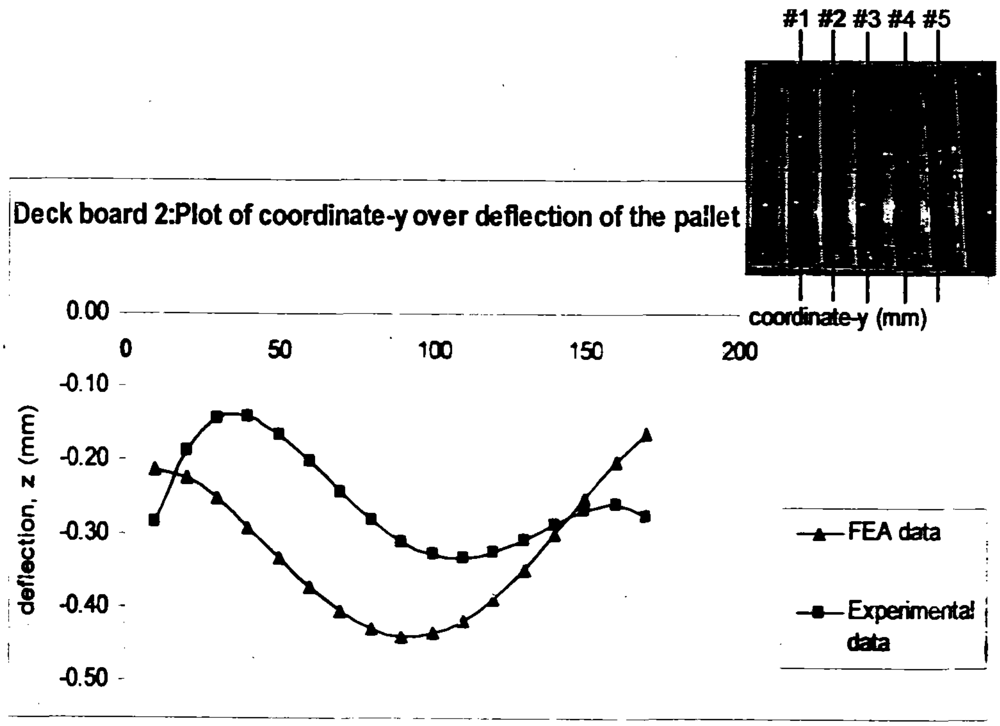

Figure 7.10(b): Comparative study of the deflection of the pallet between experimental and modeling data.

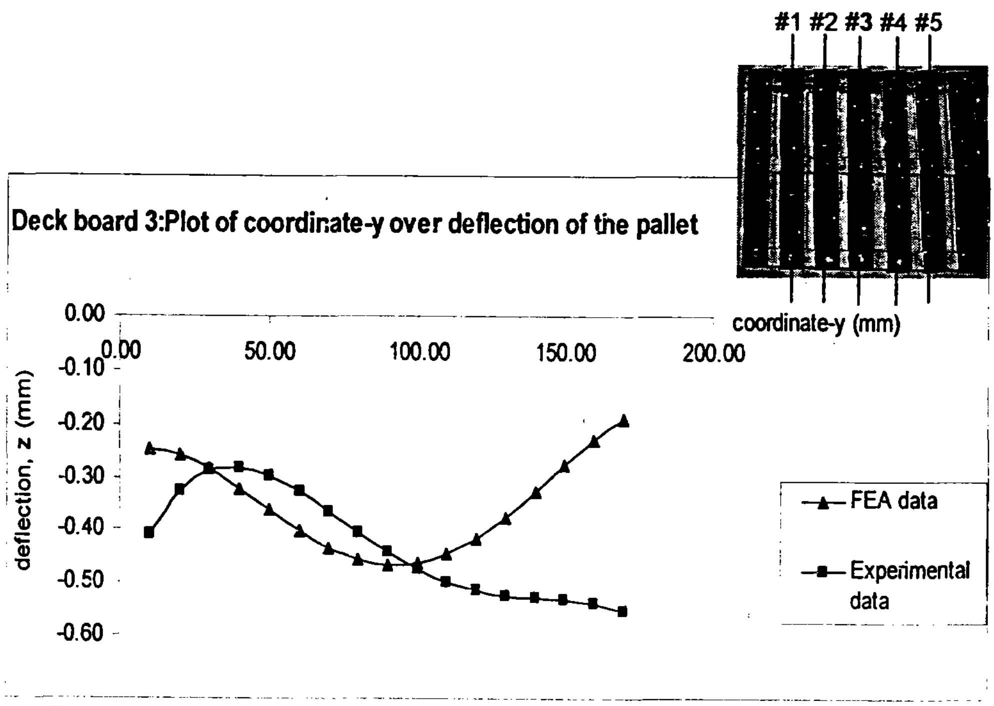

Figure 7.10(c): Comparative study of the deflection of the pallet between experimental and modeling data.

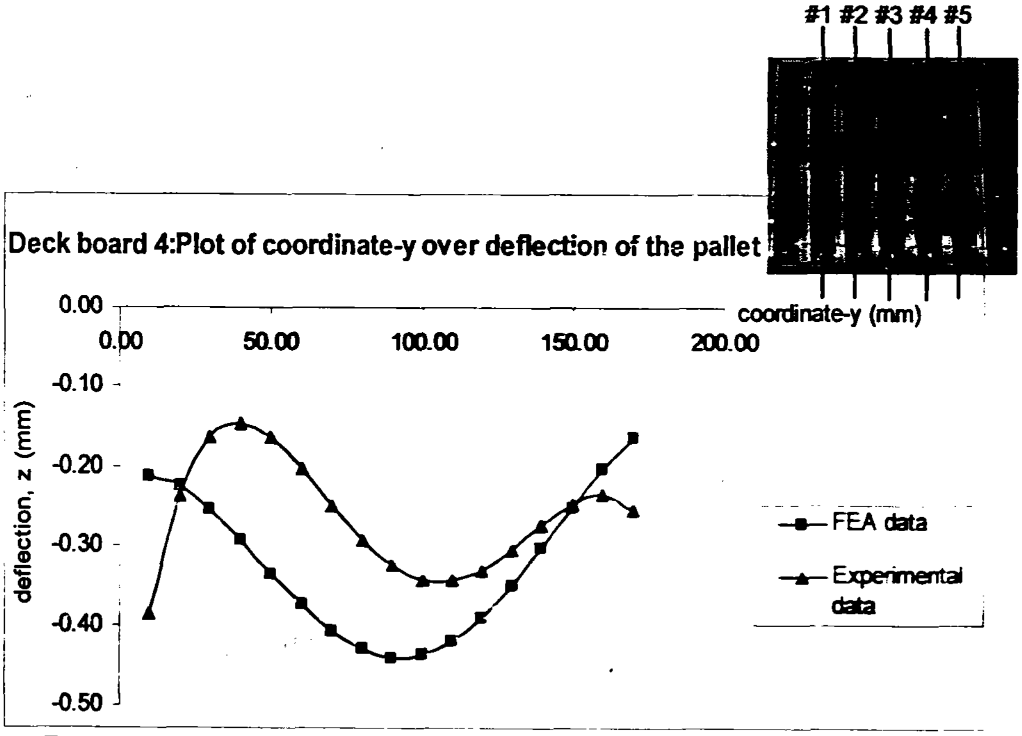

Figure 7.10(d): Comparative study of the deflection of the pallet between experimental and modeling data.

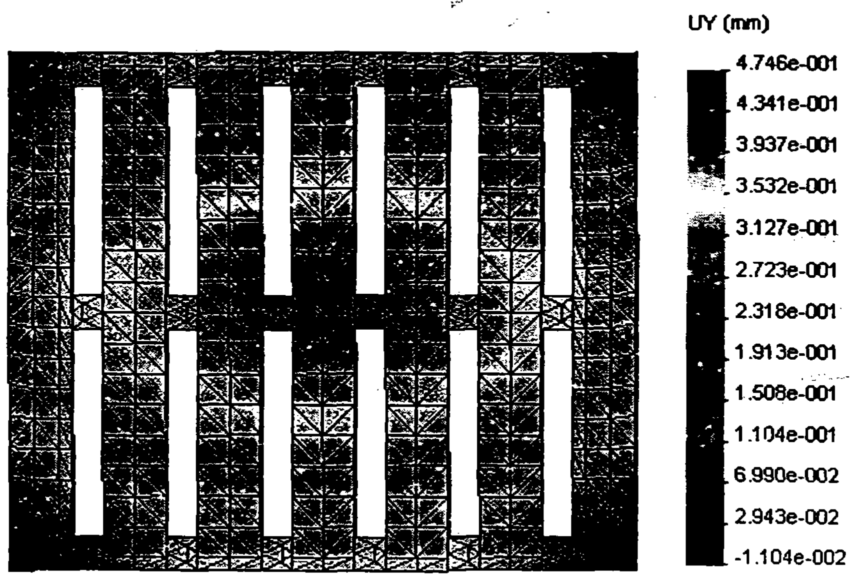

Figure 7.11: Deflection profile of pallet model in FEA analysis.

Figure 7.9(a) to (d) show that the distance measured from pallet to the grating after loading is always lower than data for pallet without loading. This is expected because the pallet will deform when center load is applied on the pallet. The comparative study of the deflection at the center of each deck board of the pallet (at x = 90.0 mm) between experimental and modeling data show that the differences between these data are small, that is 0.08 mm, 0.13 mm, 0.03 mm and 0.12 mm for deck board1, deck board 2, deck board 3 and deck board 4, respectively. In other words, when experimental and FEA data are compared, there is a close agreement at the center of the deformed pallet while the deformation at other positions of the pallet is bigger except at the center of each deck board of the pallet. For instance at deck board 3, the difference in deflection at x = 170.0 mm between experimental and modeling data is 0.36 mm. This is probably due to non-homogeneity of wood sawdust-polypropylene composite material and assumption was made in the FEA analysis.

Figure 7.10(a) shows a smooth deflection profile for both experimental and FEA results. The deformation gradient for both data shows a downward trend at left hand side of the deck board while the gradient shows a upward trend at the right hand side of the deck board, Figure 7.10(b) and (d) show a different deformation trend where the slope for experimental data shows a positive sign while slope for FEA results show a negative signs at the left hand side of the deck board. When the slope of FEA results shows a positive sign at the right hand side of the deck board, the deformation gradient of experimental data show a negative signs. Figure 7.10 (c) shows the center deck board of the pallets, at this deck board, the deformation gradient shows a positive sign on the left hand side of the deck board and negative sign on the right hand side of the deck board. It is opposite to FEA data where the slope shows a negative sign at left hand side of deck board and positive sign at right hand side of the deck board.

Once again, this is explained by the use of non-homogeneous composite material which stress do not transfer uniformly when load is applied on this composite pallet.

7.3 Summary

Dimension of one fifth scaled pallet model was modified in order to meet the requirement of nominal size of screw that was selected for the assembly of the pallet model. Wider stringers of the pallet model were used in order to avoid cracking of the pallet model while joining the deck boards to the stringer with mechanical fasteners. Comparison of deflection profile for pallet model showed that there is a close agreement between experimental and modeling data at the center of the pallet while there is a big variation of deformation at other positions except center of the pallet. This variation is probably due to the non-homogeneity of the wood based composite material.

INVENTION • INNOVATION • INDUSTRIAL DESIGN • TECHNOLOGY

I•TEX

Certificate of Award

This is to certify that

Dr Mani Maran Ratnam, Dr Abdul Khalil Shawkataly, Lim Juinn Hsuh

has been awarded the

Bronze Medal

for the Invention

Pallet from Recycled Plastic & Natural Fiber

at the
International Invention Innovation
Industrial Design & Technology Exhibition

I•TEX 2003

on **16-18 May 2003**

MINDS

Tan Sri Datuk Dr. Augustine S. H. Ong
President
Malaysian Invention and Design Society